Gondwana Research 27 (2015) 686–700

Contents lists available at ScienceDirect

Gondwana Research

journal homepage: www.elsevier.com/locate/gr

Origin of ultrahigh pressure and highly reduced minerals in podiform chromitites and associated mantle peridotites of the Luobusa ophiolite, Tibet

XiangZhen Xu [a,*], JingSui Yang [a], Paul T. Robinson [a], FaHui Xiong [a], DengZhu Ba [a], GuoLin Guo [b]

[a] State Key Laboratory of Continental Tectonic and Dynamics, Institute of Geology, Chinese Academy of Geological Sciences, Beijing 100037, China
[b] State Key Laboratory Breeding Base of Nuclear Resources and Environment, East China Institute of Technology, Nanchang 330013, China

ARTICLE INFO

Article history:
Received 6 September 2013
Received in revised form 12 May 2014
Accepted 21 May 2014
Available online 23 June 2014

Keywords:
Diamond
Mantle peridotite
Chromitite
Luobusa
Tibet

ABSTRACT

Podiform chromitites and their host peridotites in the Kangjinla mining district of the Luobusa ophiolite contain similar collections of ultrahigh pressure (UHP), highly reduced and crustal-type minerals. Abundant diamonds have been recovered from both lithologies and these are associated with a wide range of base metal alloys, native elements, carbides, oxides, silicates and others. The presence of UHP and highly reduced minerals in these rocks indicates that at least some of the chromite must have crystallized deep within the mantle as well as in a shallow mantle wedge in a suprasubduction zone (SSZ) environment. The unusual minerals were encapsulated in chromite grains and carried upward by mantle convection. The peridotite of Luobusa was trapped in the mantle wedge where it was modified by SSZ fluids and melts. Partial melting and mobilization of the chromite grains allowed them to be carried to shallow levels in melt channels and eventually deposited as chromitites near the crust mantle boundary. The unusual minerals were preserved during this process because they were encapsulated in chromite grains, either during crystallization or by later fluid fluxing.

1. Introduction

Diamonds and other ultrahigh pressure minerals were first reported in chromitites of the Luobusa ophiolite in 1981 (IGCAGS, 1981), but this discovery attracted little attention until a more detailed investigation was undertaken in 1998 (Bai et al., 2000; Yang et al., 2003; Robinson et al., 2004; Yang et al., 2007a). These initial reports were met with considerable skepticism because the diamonds were recovered from heavy mineral separates and it was impossible to rule out natural or anthropogenic contamination of the samples (Taylor et al., 1995). However, in recent years diamonds, as well as other UHP and related minerals, have been found in-situ, providing incontrovertible evidence of their natural origin (Yang et al., 2014). The mineral inclusions (Xu et al., 2011a) and trace element patterns of the diamonds (Griffin et al., 2013) clearly distinguish them from synthetic grains and most cratonic diamonds.

Podiform chromitites occur in the upper mantle sections of ophiolites, near the crust–mantle boundary, and are generally regarded as having formed at very low pressures. However, the discovery of UHP and highly reduced minerals such as diamond and coesite in oceanic chromitites (Bai et al., 1993; Yang et al., 2007a) raises important questions about the origin of ophiolites and their podiform chromitites, as well as the nature of deep mantle processes. Most of the previous work on the Luobusa ophiolite was focused on the podiform chromitites and their unusual minerals (Hu, 1999; Bai et al., 2000; Yang et al., 2003; Robinson et al., 2004; Bai et al., 2006a,b; Yang et al., 2007a; Xu et al., 2008; Yang et al., 2008a,b; Fang et al., 2009; Shi et al., 2009; Xu et al., 2009; Yamamoto et al., 2009; Li et al., 2010; Xu et al., 2013). Understanding the origin of the podiform chromitite is the key in interpreting the UHP and highly reduced minerals that they contain. In order to understand the physical and chemical conditions under which podiform chromitites form, it is necessary to determine their textures and mineralogies, as well as their relationship to the host peridotites. In this study we compared the mineralogy of podiform chromitite 11 in the Kangjinla district of the Luobusa ophiolite in order to determine whether the deep mantle minerals occur only on the chromitites or in both chromitites and peridotites. Same chromite deposit to check whether the similar deep mantle minerals can be always. Thus we report the character and mineralogy of the chromitite and peridotite orebody 11 and present a model for their formation.

2. Geological setting

The Luobusa ophiolite lies in the eastern part of the Yarlung Zangbo suture zone, which marks the tectonic boundary between Asia and India. It is located about 200 km ESE of Lhasa where it forms a body −43 km long in an east–west direction and −4 km wide, with an exposed area of −70 km^2. To the south, the ophiolite is separated from

* Corresponding author at: 26 Baiwanzhuang Road, Beijing 100037, China. Tel.: +86 10 68990674; fax: +86 10 68999698.
E-mail address: xuxiangzhensjl@aliyun.com (X. Xu).

http://dx.doi.org/10.1016/j.gr.2014.05.010
1342-937X/

Triassic flysch by a steep reverse fault, whereas to the north it is thrust over the Gangdese batholith and clastic sedimentary rocks of the Tertiary Luobusa Formation. The ophiolite is a tectonic slab composed chiefly of mantle peridotites and dunites with minor crustal cumulates and mafic dikes (Fig. 1). It hosts the largest chromite deposit in China, containing nearly 5 million tons of ore (Zhang et al., 1996). The chromitite orebodies are grouped into 3 clusters, designated from west to east, the Luobusa, Xiangkashan and Kangjinla districts (Fig. 1). Nearly all of the chromitites are hosted in mantle peridotites, which is typical of Alpine or podiform chromitite deposits (Wang et al., 1983, 1987), however, a few small bodies also occur in the transition-zone dunites. Many of the chromitites have thin envelopes of dunite. The contacts between the chromitites and dunites are typically sharp with no evidence of faulting or shearing (Wang et al., 1983, 1987), however, the dunite grades outward into the host harzburgite with increasing pyroxene (Zhou et al., 1996, 2005, 2014).

The Kangjinla mining district, which lies at an elevation of −5300 m near the eastern end of the ophiolite (Fig. 1), is about 6.5 km long and 2.3 km wide. The ore deposits are mostly vein-like or lenticular bodies of chromitite with dunite envelopes. Orebody Cr-11, the largest deposit being mined in the district, strikes about N75°W and dips 50–72°SW. It ranges from 0.3 to 10.5 m thick, averaging about 3.3 m.

The textures in orebody Cr-11 are highly variable, ranging from compact and massive to disseminated, layered, nodular, anti-nodular, irregular and deformed. Massive ore typically grades into disseminated ore (Fig. 2a), but maintains sharp contacts with the host rocks (Fig. 2b). The disseminated ores are here divided into three types, sparsely, moderately and densely disseminated, depending on the abundance of chromite. Densely disseminated chromitites are commonly coarse-grained, subhedral to anhedral, and typically grade into moderately disseminated ore on the one hand and massive ore on the other (Fig. 2c). Nodular ores are sparse and occur mainly along contacts between disseminated chromitites and mantle peridotites. Individual nodules are spherical to ovoid, range in size from 0.3 to 2.5 cm and are sometimes weakly aligned. Narrow veins of compact ore are also locally present (Fig. 2d). In the Kangjinla district, the chromitite occurs with veins, lenses, and pods associated with blocks of dunite; and its irregular contact with harzburgite (Fig. 2e). Orebody Cr-11 is mainly for open-pit mining (Fig. 2f).

Most of the chromitites are quite fresh and the chromite compositions are remarkably uniform. A total of 136 chromite grains were analyzed in 20 samples and they consist of 54.6–63.1 wt.% Cr_2O_3, 8.9–12.2 wt. % Al_2O_3 and 11.7–15.6 wt. % MgO, and are therefore classified as magnesiochromite. All of the chromite grains within the chromitites have very high Cr#s (75.6–82.7) and moderately high Mg#s (56.4–74.1) (Xu et al., 2011b). These values are consistent with those from orebody 31 of the Luobusa district (Zhou et al., 1996) and with those from the Dongqiao ophiolite in central Tibet. Note that we use the term chromite to describe individual grains and chromitite to designate orebodies formed by accumulations of chromite grains.

Orebody Cr-11 is hosted mainly in clinopyroxene-bearing harzburgite with minor dunite and lherzolite. All of the peridotites are quite fresh with generally less than 5% serpentinization and their original textures and structures are well preserved. The harzburgite is medium- to coarse-grained, greenish-gray in color, and has a thin, buff-colored weathering rind. Large orthopyroxene crystals are prominent on the weathered surface and show a crude foliation, making it easy to distinguish these rocks from dunite. The harzburgite consists chiefly of forsteritic olivine (75–90 modal%), Mg-rich orthopyroxene (7–25%), minor clinopyroxene (2–3%) and accessory minerals such as magnetite and residual chromite (1–2%). Sparse secondary minerals include serpentine, brucite, magnesite and chlorite.

Small amounts of lherzolite are also locally present, being characterized by 5–10 modal% clinopyroxene. The clinopyroxene grains are small (<1 mm) and interstitial to the granular olivine. Orthopyroxene in these rocks typically forms short, prismatic grains with many clinopyroxene exsolution lamellae and undulatory extinction.

Dunite occurs chiefly as envelopes around the orebodies or as patches and zones interspersed with the chromite ore. Some small lenses of dunite also occur locally in the peridotites. These dunite lenses are distinct from the thick, transition-zone dunite at the base of the ophiolite, and show very complicated relationships with the chromitite

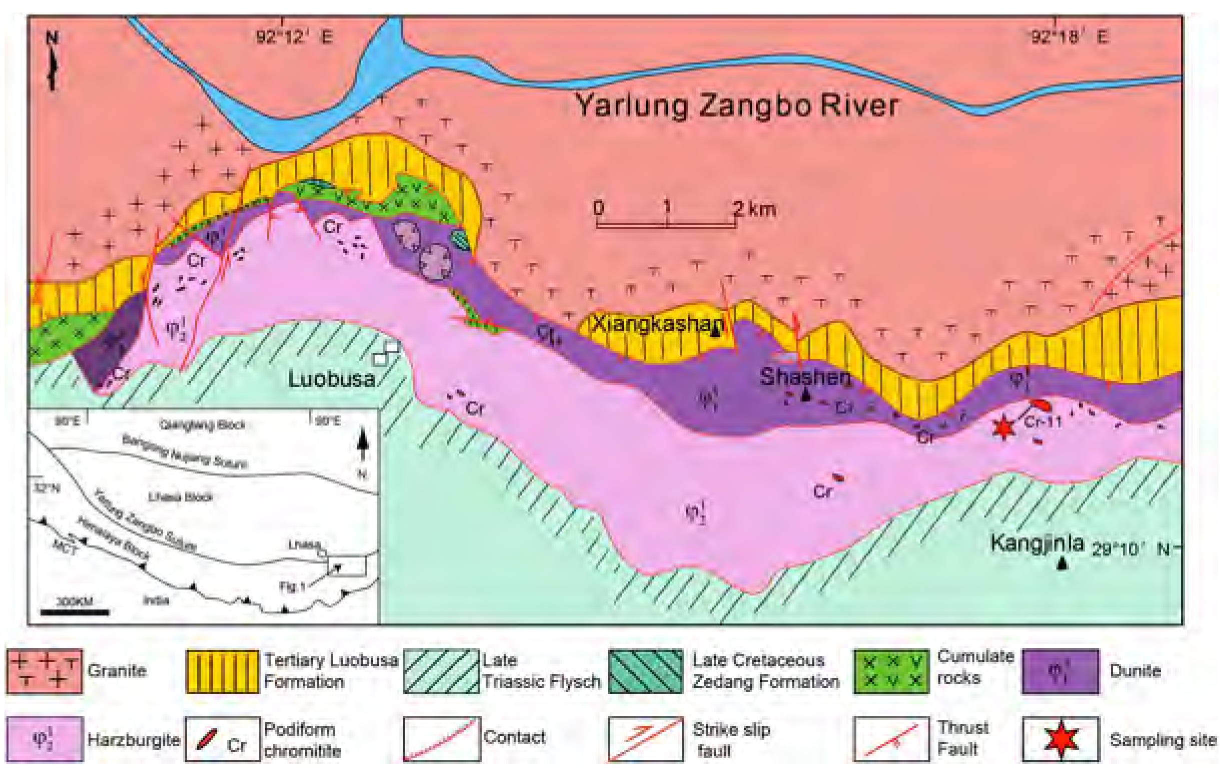

Fig. 1. Simplified geological map of the Luobusa ophiolite, Tibet.
Revised after Zhou et al. (1996).

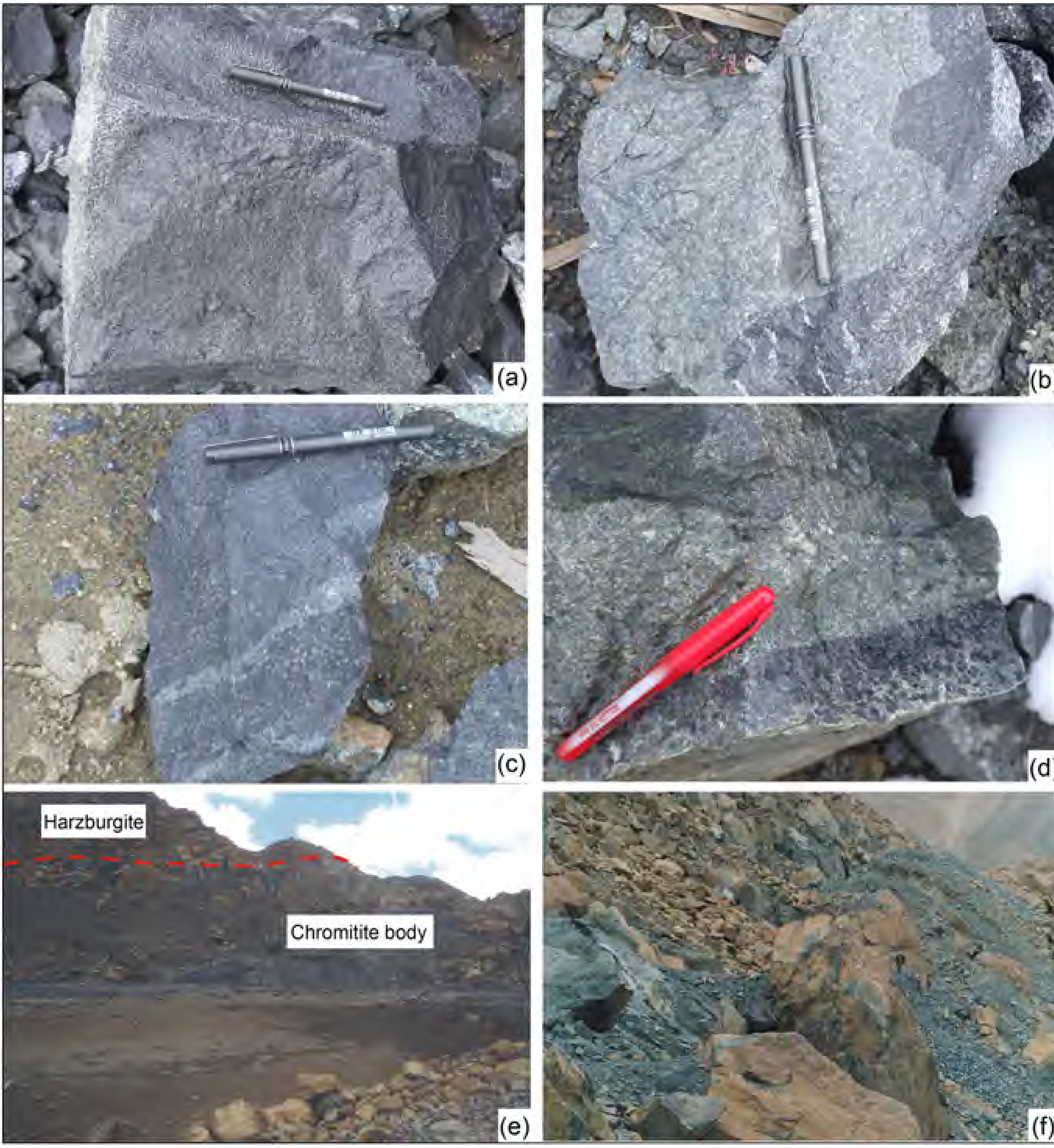

Fig. 2. Photographs showing the textures and structures of chromitite from orebody Cr-11 in the Kangjinla mining district of the Luobusa ophiolite. (a) Chromitite with massive ore and disseminated ore; (b) a sharp contact between massive chromitite and the host mantle peridotite; (c) chromitite with moderately to dense disseminated and massive ore; (d) contact between layered chromitite and dunite; (e) the view of the orebody Cr-11 and its irregular contact with harzburgite; (f) orebody Cr-11 by open-pit.

ores, commonly being broken into blocks that both contain abundant chromite nodules and are surrounded by disseminated ore (Robinson et al., 2004). The blocks have different sizes and shapes and generally display sharp contacts with the ore. In thin section, the dunite displays granular textures, sometimes with evidence of plastic deformation and recrystallization. Typical samples consist of >95 modal% olivine, 1–2% magnesiochromite and traces of orthopyroxene and clinopyroxene.

Most of rock-forming minerals in the peridotites and dunites show at least two stages of formation; an early stage of relatively large, commonly deformed, crystals and a second stage of smaller, undeformed but recrystallized grains. The compositions of the minerals show some variations between the stages. First-stage olivine has relatively low Fo values, orthopyroxene and clinopyroxene have high Al_2O_3 and Cr_2O_3 contents, and magnesiochromite has low Cr#s, whereas second-stage minerals show the opposite trend. Olivine in the chromitites is very

Mg-rich ($Fo_{96–97}$), significantly higher than that in the host peridotites ($Fo_{90–92}$) and dunites ($Fo_{92–94}$), presumably reflecting subsolidus re-equilibration between chromite and olivine (Xu et al., 2011b).

Residual magnesiochromite grains in the mantle peridotites have Cr#s ranging from 29.8 to 76.9 and Mg#s ranging from 39.4 to 70. They plot in the abyssal and island-arc fields in the Cr# vs. Mg# diagram (Dick and Bullen, 1984), probably reflecting different degrees of partial melting and melt–rock reaction rather than formation in different tectonic environments (Xu et al., 2011b).

3. Sampling and processing

To test whether the Kangjinla chromitites and their host peridotites contain similar UHP other minerals we collected two samples; one consists of 1116 kg of massive chromitite from orebody Cr-11, the other is a 384-kg sample of peridotite collected immediately adjacent to the chromitite. Mineral separation was carried out at the Institute of Multipurpose Utilization of Mineral Resources, Chinese Academy of Geological Sciences, Zhengzhou. The samples were first passed through a jaw crusher and then ground in stages to three sizes: <1 mm to >0.5 mm, <0.5 mm to >0.3 mm, and <0.3 mm. Minerals were separated from each size fraction by a combination of gravity, magnetic and electrostatic techniques in order to obtain grains of different sizes and densities. Before processing, all worksites and equipment were carefully cleaned to avoid any contamination. Details of the mineral separation procedures are given in Xu et al. (2009).

Concentrates from each size fraction were handpicked under a binocular microscope, and the selected minerals were mounted in epoxy and ground to approximately half their thickness. The grains were polished using grinding paste and then cleaned in an ultrasonic bath. The procedure is similar to that for preparation of zircon dating samples. The selected minerals were analyzed with a S-3500N scanning electron microscope (SEM) with an energy-dispersive spectrometer at the Beijing General Research Institute of Mining and Metallurgy, and a JEOL JSM-5610LV SEM with an energy-dispersive spectrometer, a RENISHAW-1000 Laser Raman, and an X-ray diffraction instrument in the State Key Laboratory of Continental Tectonic and Dynamics, Chinese Academy of Geological Sciences, Beijing. The SEM was operated at a voltage of 20 kV and a beam current of 15 nA, and cobalt metal was used for calibration. The X-ray diffraction analyses were carried out at a voltage of 30 kV and a beam current of 20 mA. X-ray photographs were exposed for 6 h and interpreted using the reference data in the X-ray Mineral Powder Identification Manual edited by the Institute of Geochemistry, Chinese Academy of Sciences. A number of minerals were also analyzed using a JXA-8100 electron microprobe with an Inca energy-dispersive spectrometer in the State Key Laboratory of Nuclear Resources and Environment, East China Institute of Technology. This electron microprobe was operated at a voltage of 15 kV, with a beam current of 1.0×10^{-8} A, and a spot diameter of 1 μm.

4. Diamonds and other exotic minerals in the mantle peridotite

The mantle peridotite at Kangjinla consists of 75–90 modal% olivine, 7–25% orthopyroxene, <3% clinopyroxene and 1–2% magnesiochromite. In thin section, the olivine occurs as colorless, transparent, generally granular aggregates with an average composition of Fo_{94}. Orthopyroxene forms large tabular crystals with an average composition of En_{90} and Cr_2O_3 contents up to 0.72%. Both CaO and Al_2O_3 contents are low, as expected for orthopyroxene in mantle peridotite. The clinopyroxene is all diopside, which occurs as both small, interstitial grains and as exsolution lamellae in the orthopyroxene.

Numerous exotic mineral species were recovered from the mantle peridotite, including native elements, carbides, alloys, oxides, sulfides, silicates, carbonates and others (Table 1).

4.1. Native elements

Native elements recovered from the peridotite include diamond and native iron. Diamonds are particularly abundant; more than 1000 grains of diamond have been recovered thus far from the 384-kg sample. The diamonds are all pale yellow to colorless, euhedral to subhedral crystals, 200–500 μm across, with octahedral, cuboctahedral, and dodecahedral morphologies (Fig. 3a, b). Some grains are single crystals, whereas others are polycrystalline (Fig. 3c) or skeletal (Fig. 3d). Dozens of analyzed grains yielded characteristic Raman patterns with a shift at 1332.6 cm^{-1} (Fig. 3e). An examination of their energy spectra indicates that the diamonds are composed of pure carbon.

Native iron occurs as small, gray spheres, generally 150–500 μm in diameter. Single crystal X-ray diffraction data for one particle (Fig. 4a) are listed in Table 2. The native iron is α-Fe.

Wüstite (FeO) commonly rims the spheres of native iron or occurs as inclusions within them (Fig. 4b, c). These features are similar to those of native iron and wüstite in the Luobusa chromitite (Bai et al., 2006a; Xu, 2009). The chemical compositions of native iron and wüstite are quite simple, although some wüstite grains contain a small amount of Ti (Table 3, Ky-6-2-8-1-3). The boundaries between the native iron and wüstite are very sharp, indicating that they did not form by replacement or diffusion.

4.2. Carbides

Carbides recovered from the peridotite sample are mainly moissanite, which is similar to that recovered from chromitite of orebody 31 (Robinson et al., 2004; Trumbull et al., 2009). Moissanite occurs as subhedral, hexagonal crystals (Fig. 5a) or rounded grains (Fig. 5b), typically 0.1–1.0 mm in diameter. It varies from colorless to light green, bluish-green to deep blue. All analyzed grains have typical Raman patterns with shifts at 790, 972, and 768 cm^{-1} (Fig. 5c). The composition includes minor N, as shown in Table 3 (Ky-7-3-19.1).

4.3. Alloys and oxides

Most alloys recovered from the peridotite consist of Fe–Ni, Ni–Mn–Co, and Fe–Cr–Ni, and these are both less varied and less abundant than those in the chromitite. Fe–Ni alloys are rare in the peridotite and may be associated with serpentine (Fig. 6). The alloy associated with serpentine has a formula of $Fe_{2.8}Ni_{7.2}$ (Table 3, Ky-6-5-5.1). The composition of the serpentine is given in Table 4 (Ky-6-5-5.2).

Table 1
Mineral assemblages recovered from the chromitites and host peridotites in the Kangjinla orebody Cr-11, Tibet.

	Chromitite	Mantle peridotite
Wt. of sample	1116 kg	384 kg
Native elements	Diamond, native iron, tantalum	Diamond, native iron
Carbides	Moissanite	Moissanite
Alloys	Fe–Ni, Fe–Ni–Cr, Mn–Ni, Fe–Cr, Fe–Si, P–Si–Ti, Ti–Si, Co–Mn–Ni	Fe–Ni, Ni–Mn–Co, Fe–Cr–Ni
Oxides	Wüstite, hematite, magnetite, periclase, chromite, rutile, ilmenite, corundum and other complex oxides	Wüstite, hematite, magnetite, periclase, chromite, r utile, ilmenite, cassiterite, bismuth oxide, quartz and other complex oxides
Other minerals	Sulfides, silicates, tungstates and carbonate minerals	Sulfides, silicates, tungstates and carbonate minerals

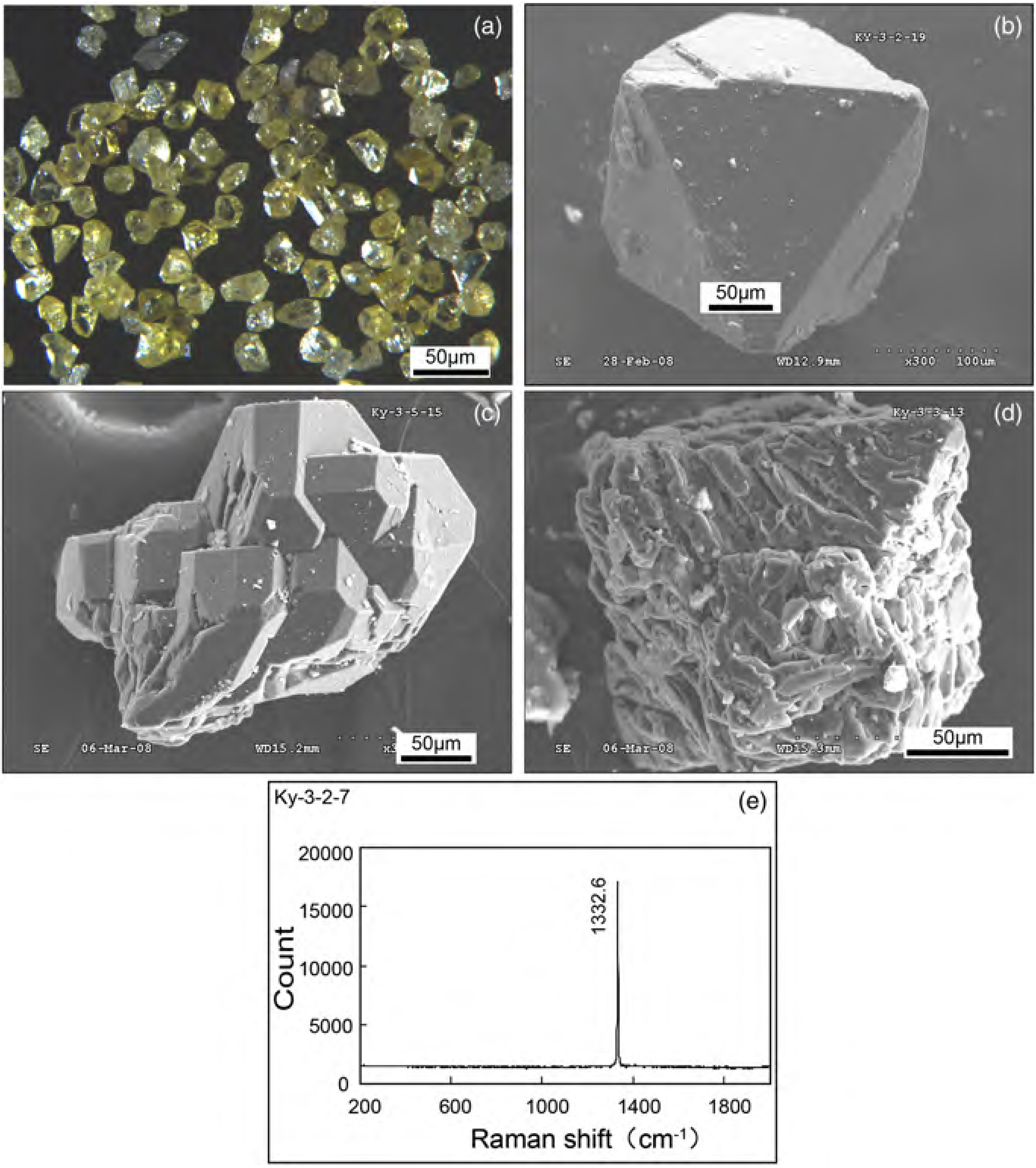

Fig. 3. Photographs showing diamonds recovered from the Kangjinla peridotite hosting orebody Cr-11. (a) Microphotograph showing abundant yellow diamonds; (b) SE images showing octahedral diamond; (c) SE image showing diamonds with polycrystalline; (d) SE image showing the skeletal structure of diamond; (e) Raman spectrogram showing characteristic shift at 1332.6 cm^{-1}.

Numerous oxides were recovered from the peridotite (Table 1). Most are Fe, Ti or Cr oxides but cassiterite, bismuth oxide, and other complex oxides are also present.

Wüstite was described above in connection with native Fe and is not discussed here.

Magnetite occurs as black spheres or ovoids. Magnesiochromite is common in the peridotite sample but rarely exceeds 2 modal%. It forms irregular black grains, generally 1–2 mm in diameter, with an average Cr# of 79.4 and Mg# of 71.4. The Cr# of these grains is very close to that of magnesiochromite in the adjacent chromitite and much

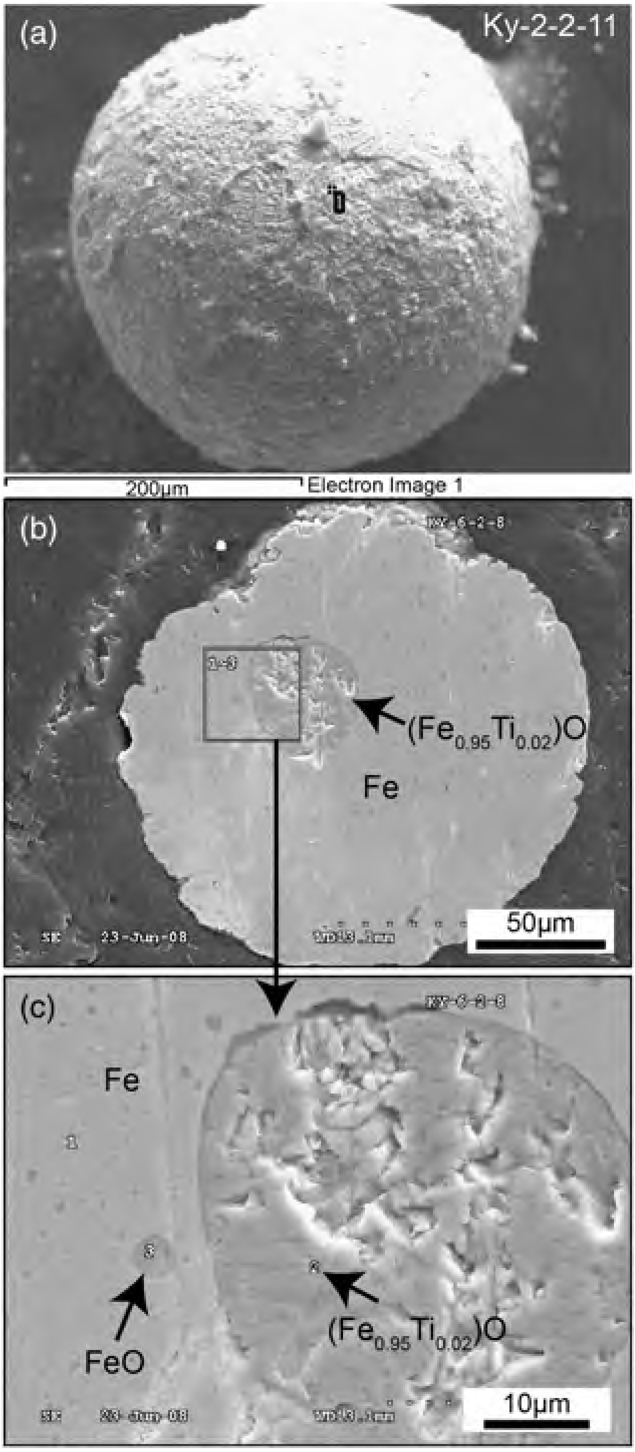

Fig. 4. Photographs showing the characteristics of native iron and wüstite in the Kangjinla peridotite. (a) Electron image showing sphere of native iron; (b) SE image showing sphere of wüstite inclusion (darker gray) in native Fe (light gray); (c) enlarged segment of (a), SE image showing inclusions of FeTiO and FeO in native iron.

higher than residual magnesiochromite elsewhere in the peridotites. This implies that these grains have been modified by melts from which the podiform chromitite formed. These grains are commonly associated with olivine (Table 4, Ky-6-5-1.1-1.2), which has a composition of $Fo_{97.6}$ and contains up to 0.86 wt.% NiO.

Rutile occurs as irregular to columnar, red, transparent to translucent grains, commonly 200–300 μm but up to 550 μm long. It also occurs as small (10 μm) inclusions in pyrite. Most grains contain 1.5–2 wt.% Fe (Table 4, Ky-7-6-13.2).

Table 2
Representative X-ray diffraction data for native iron in the Kangjinla peridotite.

D (Å)	I	D (Å)	I
(2.23)	4	(1.292)	2
2.024	10	1.170	8
(1.580)	1	1.013	6
1.433	6		

Note: the reference data are from the X-ray Mineral Powder Identification Manual edited by the Institute of Geochemistry, Chinese Academy of Sciences (card number 13).

4.4. Other minerals

In addition to the minerals mentioned above, small amounts of almandine garnet, andalusite, zircon, feldspar, chlorite and serpentine together with olivine, clinopyroxene, and orthopyroxene were also recovered. The chlorite and serpentine are clearly alteration minerals, whereas the olivine, clinopyroxene and orthopyroxene are the primary minerals of the peridotite.

Of particular interest is the andalusite, which forms light yellow, transparent, irregular to columnar grains, 600 μm long and 200 μm wide. Microprobe data indicate that the andalusite is nearly pure Al_2O_3 and SiO_2 with a small amount of FeO (Table 4, Ky-7-2-5.1).

5. Diamond and other exotic minerals in the chromitite

More than 40 mineral species were recovered from the chromitite of orebody Cr-11 (Table 1). The most common and important include native elements (diamond, Fe, Ta), a wide range of base metal alloys, carbides (moissanite), numerous Fe, Mg, Ti and Al oxides, and sulfides, silicates, tungstates and carbonates.

5.1. Native elements

Native elements recovered from orebody Cr-11 are mainly diamond, native iron and native tantalum, a much simpler collection than that recovered from orebody Cr-31 (Bai et al., 2000; Robinson et al., 2004). More than 1000 diamond grains were recovered from the 1116-kg sample from Kangjinla. These are generally pale yellow to colorless, euhedral crystals, 200–500 μm across, with octahedral (Fig. 7a, b), cuboctahedral, and dodecahedral forms. Some grains are polycrystalline (Fig. 7c), whereas others show zircon attached to the surface of diamond (Fig. 7d). More than 20 analyzed grains yielded characteristic Raman patterns with a shift at 1332.6 cm^{-1}. Inclusions are rare in these diamonds and consist mostly of alloys such as Co–Mn–Ni, Cr–Fe, and Fe–Si and native elements such as Fe and Ta (Xu et al., 2008, 2009).

More than 100 grains of native iron were recovered from orebody Cr-11, and they occur as small spheres, generally 150–500 μm in diameter. Wüstite forms rims on some of the spheres (Fig. 8) and can also occur as very small, spherical inclusions in the native iron. The native iron and wüstite generally have simple compositions, but some grains include very small quantities of Mn, Ti and Si.

5.2. Alloys

Alloys recovered from the chromitite are Fe–Ni, Ti–N, Fe–Ni–Cr, Mn–Ni, Fe–Cr, Fe–Si, Ti–Si–P, Ti–Si, Ti–C, Ti–B–N–C, Si–Ti–Ni, and Co–Mn–Ni. Surprisingly, most of these occur as inclusions in corundum, except for the Fe–Ni alloys.

The Fe–Ni alloys are spherical grains or elongate rods, gray-black in color and about 1.0 mm across. They have a formula of $Fe_{2.6}Ni_{7.4}$ (Xu et al., 2009) and their identification is confirmed by single crystal X-ray diffraction data (Table 5). Inclusions such as pentlandite, periclase and magnesium silicate are common in these grains, and some of the alloys occur as inclusions within magnesiochromite grains (Xu et al., 2009). These alloys are sometimes accompanied by small (−20 μm long), droplet-shaped inclusions of Ni–Fe sulfides (Fig. 9a; Table 3). The host

Table 3
Composition of the special minerals in the Kangjinla peridotite and chromitite.

Sample no.	Composition (wt.%)																Formula
	Fe	O	Ti	Si	N	C	Ni	As	Co	Te	Pb	Cu	Se	S	Mo	Total	
Ky-6-2-8-1	100															100	Fe
Ky-6-2-8-2	75.7	22.73	1.57													100	$(Fe_{0.95}Ti_{0.02})O$
Ky-6-2-8-3	77.73	22.27														100	FeO
Ky-7-3-19.1	0.02			69.78	0.4	28.52	0.02									98.74	$N_{0.1}C_{4.9}Si_5$
Ky-6-5-5.1	26.62						70.89	0.05	0.23	0.11	0.04	0.27				98.21	$Fe_{2.8}Ni_{7.2}$
KCr-9-3-8.3	2.90						69.45			0.17	–	0.08	–	25.77	0.40	98.77	$(Fe_{0.1}Ni_{2.9})_3S_2$
KCr-9-3-8.4	32.65						33.41		0.28	0.09		0.09	0.06	32.76	0.37	99.70	$(Ni_{4.5}Fe_{4.5})_9S_8$

Note: "–" = below detection limit. KCr-9-3-8.3 is a heazlewoodite and KCr-9-3-8.4 is a pentlandite.

magnesiochromite grains are rich in both Cr_2O_3 (59.9 wt.%) and MgO (14.9 wt.%), yielding a Cr # number of 78.2, and a Mg# number of 71.16 (Table 4, KCr-9-3-8.1).

5.3. Other minerals

A few moissanite grains were recovered from the chromitite sample. They form flat, hexagonal crystals, generally 0.1–1.0 mm in diameter, that range from colorless, to light green and bluish-green to deep blue. Analyzed grains all have typical Raman patterns with shifts at 790, 968 and 767 cm^{-1} (Xu et al., 2009).

Oxides recovered from the podiform chromitite are mainly wüstite, hematite, magnetite, periclase, chromite, rutile, ilmenite and corundum. The wüstite was described above and is not discussed further here. Hematite generally forms perfect iron gray spheres (Fig. 9b). Periclase occurs as small inclusions in Fe–Ni alloys (Xu et al., 2009). Rutile is relatively common in the chromitite, where it forms small, reddish, irregular prisms, mostly 200–300 μm long. One grain has an ovoid inclusion of zircon about 100 μm across and a small inclusion of ilmenite (Xu et al., 2009).

Magnesiochromite grains are mostly 1–2 mm across and black in color. Numerous, relatively large (>1 mm), irregular, pinkish grains of corundum were also recovered. They consist of almost pure Al_2O_3, but contain many inclusions, such as rutile and a variety of alloys, including Ti–N, Ti–Si, Ti–C, Ti–Si–P, Ti–B–N–C, and Si–Ti–Ni and some REE-bearing silicates (Xu et al., 2013). Small (up to 25 μm), highly reflective inclusions of unknown materials are also present in some grains. They consist of Ti, Zr, Al and O and are intergrown with a P–N–Si–Ti alloy (Table 4) (KCr-10-5-1.1, KCr-10-5-1.3, KCr-10-5-6.1, KCr-10-5-6.4, KCr-10-5-6.5, KCr-13-1-3.2). This mineral has not been reported before in the Luobusa chromitites and further research will be performed to determine its structure and composition. Some inclusions of TiN also occur in the corundum (Xu et al., 2013).

Other minerals include garnet, andalusite, zircon, sphene, and feldspar. The garnet forms salmon pink grains composed of 50% almandine, 27% grossular, 22% pyrope, and 1% spessartite.

6. Fourier transform infrared (FTIR) spectroscopy of diamonds from the mantle peridotite and chromitite

Natural diamonds usually contain nitrogen from a few to several thousand ‰, which occurs as A, B, C, and D defects (or centers); the presence of nitrogen is recorded by elevated absorption within 900–1400 cm^{-1} wavelength numbers range at IR spectra (Dobrzhinetskaya, 2012). The process involves the incorporation of the singly substituted N atoms (e.g., C-defects) in Type Ib diamonds (Chrenko et al., 1977). With time, single N atoms merge to pairs called A centers (Type IaA diamonds). Further diffusion and aggregation of the nitrogen follow formation of four N atoms plus a vacancy (Type IaB diamonds). In kimberlites and lamproites, most diamonds (>95%) are xenocrysts that formed earlier in rocks equilibrated in Earth's mantle (Richardson et al., 1984). Data show that 99.9% are of the IaA–IaB type (Cartigny et al., 1997, 2003), whereas diamonds from ultrahigh pressure metamorphic (UHPM) terranes belong to mixed Type Ib–IaA (e.g. Taylor et al., 1990; Finnie et al., 1994; Dobretsov et al., 1995; Cartigny et al., 2001; Dobrzhinetskaya et al., 2006).

We performed infrared measurements of the ophiolite diamonds at the Laboratoire de Géochimie des Isotopes Stables, Institut de Physique du Globe de Paris. Mid-infrared absorption spectra were first obtained using a Digilab UMA300 IR microscope attached to a Digilab FTS-20/80 FTIR spectrometer; subsequent measurements were made using a Nicplan IR microscope attached to a Nicolet 6700 Magna-IR FTIR spectrometer. Infrared spectra were deconvoluted into their different components with a precision of $\pm 2.5\%$ using coefficients of 16.5 at. ppm cm^{-1} for A (Boyd et al., 1994) and of 79.4 at. ppm cm^{-1} for B (Boyd et al., 1995a). Nitrogen concentrations were selected after the FTIR measurements. They were analyzed using the procedure described by Boyd et al. (1995b).

We selected clean, large, transparent and flat diamonds from the mantle peridotite and chromitite in the Tibet. We analyzed 21 diamonds from the chromitite and 18 diamonds from the mantle peridotite; some spectra are shown in Fig. 10. All the IR spectra are virtually identical, and are dominated by strong absorption at 1130 cm^{-1} (Fig. 10). The peak at 1130 cm^{-1} is indicative of a significant presence of singly substituted nitrogen (Type Ib). These diamonds therefore are classified as transitional Type Ib. The nitrogen contents in the Kangjinla chromitite range from 152 to 428 ppm, whereas in the mantle peridotite is 151–589 ppm. Previous analyses of two diamonds from the Luobusa chromitite are IaA–IaB (Bai et al., 2001), whereas three diamonds from the Luobusa mantle peridotite are IaA (Rong et al., 2013). According to our data, there is a significant difference in IR spectra of the ophiolite-hosted diamonds and those from kimberlites and UHPM terranes. Likewise these diamonds are different in their carbon isotopes ($\delta^{13}C = -18$ to -28‰), trace elements and mineral inclusions from most diamonds occurring in kimberlites, UHP metamorphic belts and impact craters (Griffiin et al., 2013).

7. Discussion

Our study shows that UHP and highly reduced minerals are widespread in the ophiolite and, more importantly, that they occur in both the chromitites and peridotites. A comparison of mineral concentrates from the chromitite and peridotite shows that they have very similar mineral collections (Table 6), varying mostly in relative proportions of individual phases.

Because we investigated mineral separates and because there are no obvious equilibrium assemblages in these rocks, it is impossible to apply typical geothermometry and geobarometry to determine temperatures and pressures of mineral formation. Thus, we have to rely on limited information regarding individual minerals.

The only definite UHP mineral recovered in this study is diamond. Moissanite and some of the other highly reduced phases may have also formed at depth but their crystallization is controlled largely by the ambient fO_2, rather than pressure. The diamonds in the chromitites and peridotites presumably formed at depths > 150 km, the lower stability limit for diamond. Although the ophiolite-hosted diamonds are associated with many highly reduced phases, they may not have

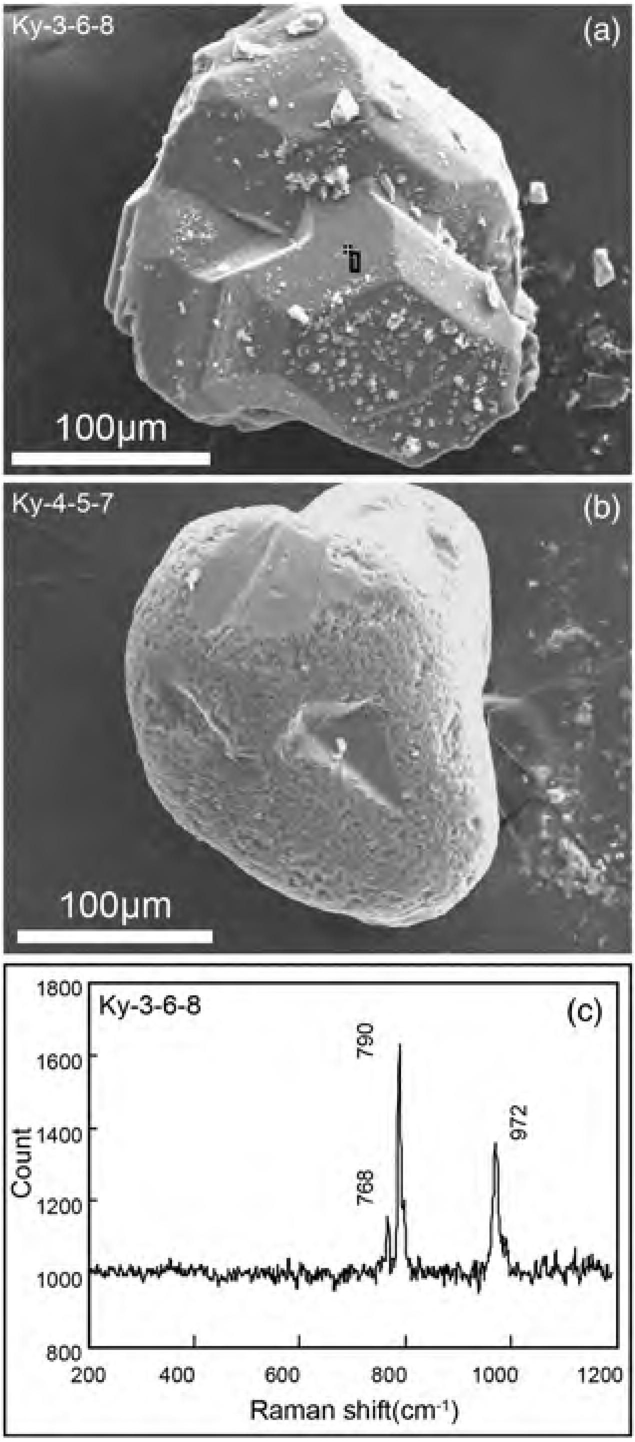

Fig. 5. Photographs showing the characteristics of moissanite in the Kangjinla peridotite. (a) SE image showing hexagonal moissanite; (b) SE image showing rounded moissanite; (c) Raman spectrum showing characteristic shifts at 790, 972, and 768 cm^{-1}.

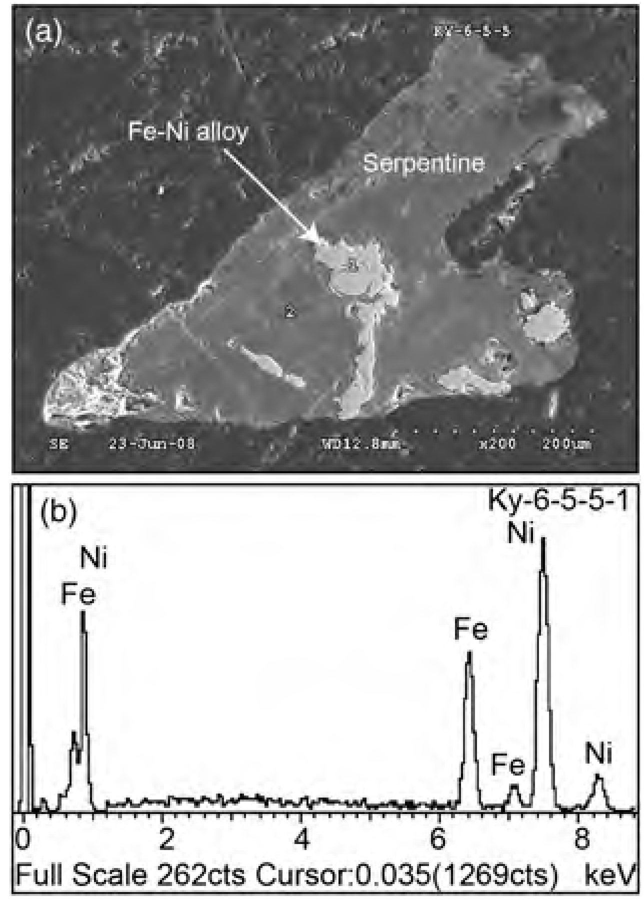

Fig. 6. Photographs showing the characteristics of Fe–Ni alloy in the Kangjinla peridotite. (a) SE image showing Fe–Ni alloy intergrown with serpentine; (b) energy spectrum showing Fe–Ni alloy in (a).

required especially reducing conditions to form; in subcontinental mantle diamond is stable at P > 4.5 GPa and fO_2 equivalent to 1–5 log units below the fayalite–magnetite–quartz (FMQ) buffer. There is abundant evidence that both chromitites and peridotites are formed in suprasubduction zones although they may have gone through several stages before their final emplacement (e.g. MacLeod et al., 2013; Rollinson and Adetunji, 2013a,b), so the presence of diamond in these rocks implies that the formation of ophiolites and their chromitites involves many steps. We suggest that the chromite grains crystallizing at above the transition zone encapsulated UHP and highly reduced minerals that were presumably present at these depths. These chromite grains were carried upward by rising peridotite and eventually placed in a suprasubduction zone wedge where the ophiolite formed. There is abundant evidence that chromite grains in suprasubduction wedges are modified, redistributed, and deposited by hydrous melts/fluids (Zhou et al., 1996).

7.1. Comparison of UHP and highly reduced minerals from the Kangjinla mantle peridotite and Purang mantle peridotite

After the discovery of diamonds and other unusual minerals in peridotites of the Luobusa ophiolite, Tibet it became important to determine if this was an isolated occurrence or if the same minerals occur in other ophiolites of the Yarlung-Zangbo suture zone. Thus, our group selected another large ultramafic massif at Purang in this belt for a comparative study. The Purang mafic–ultramafic body lies in the westernmost part of the Yarlung-Zangbo suture zone, more than 1000 km from the Luobusa massif, where it consists chiefly of mantle harzburgite with lesser amounts of lherzolite, dunite, pyroxenite and gabbro. The mineralogy and geochemistry of the Purang peridotites suggest that they formed originally at a mid-ocean ridge (MOR) and were later modified by suprasubduction zone (SSZ) melts/fluids (Xu et al., 2011b; Xiong et al., 2013), and thus they are similar to the Luobusa peridotites in their tectonic setting (Xu et al., 2011a).

Yang et al. (2011) reported the discovery of a similar collection of minerals in mantle peridotites of the Purang ophiolite (Table 6). More than 40 grains of diamond and some unusual minerals such as moissanite were recovered by standard mineral separation techniques from a 657-kg-sample of harzburgite.

Table 4
Composition of oxides and silicates in the Kangjinla peridotite and chromitite.

Sample no.	Composition (wt.%)														Name
	Na_2O	NiO	K_2O	Al_2O_3	FeO	CaO	SiO_2	MnO	P_2O_5	MgO	Cr_2O_3	TiO_2	ZrO_2	Total	
Ky-6-5-5.2	0.01	0.28	0.01	0.17	1.44	0.01	41.68	0.01	0.05	39.43	0.11			83.2	Serpentine
Ky-6-5-1.1	0.03	0.2	0.02	10.39	14.26		0.18	0.25	0.02	15	59.67	0.12		100.13	Chromite
Ky-6-5-1.2	0.19	0.86	0.18	0.05	2.37		41.78	0.02	0.03	55.04	0.2	0.05		100.77	Olivine
Ky-7-6-13.2	0.02		0.01	0.02	1.85	0.01	0.02			0.02	0.15	97.21		99.31	Rutile
Ky-7-2-5.1	0.01	0.03		62.07	0.26		37.58	0.02		0.05		0.08		100.08	Andalusite
KCr-9-3-8.1	–	0.16	–	11.22	13		0.08	0.29	0.01	15	59.94	0.2		99.65	Magnesiochromite
KCr-10-5-1.1	0.01	–		101.2		–	0.02	0.01		0.01	0.03	0.86	–	102.1	Corundum
KCr-10-5-1.3	0.01	0.01		19.74		0.27	1.59	0.01		1.52	0.07	51	27.5	101.6	(Ti, Zr, Al)O
KCr-10-5-6.1	0	0.02		95.93		0.01	0.23	0.04		0.03	0.02	1.06	0.04	97.38	Corundum
KCr-10-5-6.4	–	0.04		18.08		0.31	1.51	–		1.13	–	52.3	26.4	99.78	(Ti, Zr, Al)O
KCr-10-5-6.5	0.03	–		18.21		0.26	1.39	0.04		1.01	0.01	51.6	28.4	100.9	(Ti, Zr, Al)O
KCr-13-1-3.2	–	0.06		18.18		0.34	1.52	0.02		1.33	0.03	51.6	26.3	99.29	(Ti, Zr, Al)O

Note: "–" = below detection limit.

SEM images of diamonds (Fig. 11a, b), indicate that they have the same size (100–200 μm) and morphology as those in Luobusa and, thus are different from most kimberlite (Field et al., 2008) and UHP metamorphic diamonds (30–50 μm) (Ogasawara, 2005). More detailed work has shown that these diamonds have C isotope compositions and trace compositions as the Luobusa grains (Griffin et al., 2013; Yang et al., 2014). Combined with the new IR spectra we propose a new occurrence of diamond, called ophiolite-hosted diamond.

The presence of native Cr, Fe and Zn, together with moissanite (Table 6), indicates a strongly reducing environment. This discovery confirms that the Luobusa massif is not unique in the Yarlung-Zangbo suture. Recent experimental work has demonstrated that ferrous ions will dissociate into ferric ions + Fe metal under lower mantle conditions (Frost et al., 2004; McCammon, 2005; Rohrbach et al., 2007). These finding suggest that only the outermost layer of Earth (maybe as thin as ~250 km (Rohrbach et al., 2007)) is intensively oxidized.

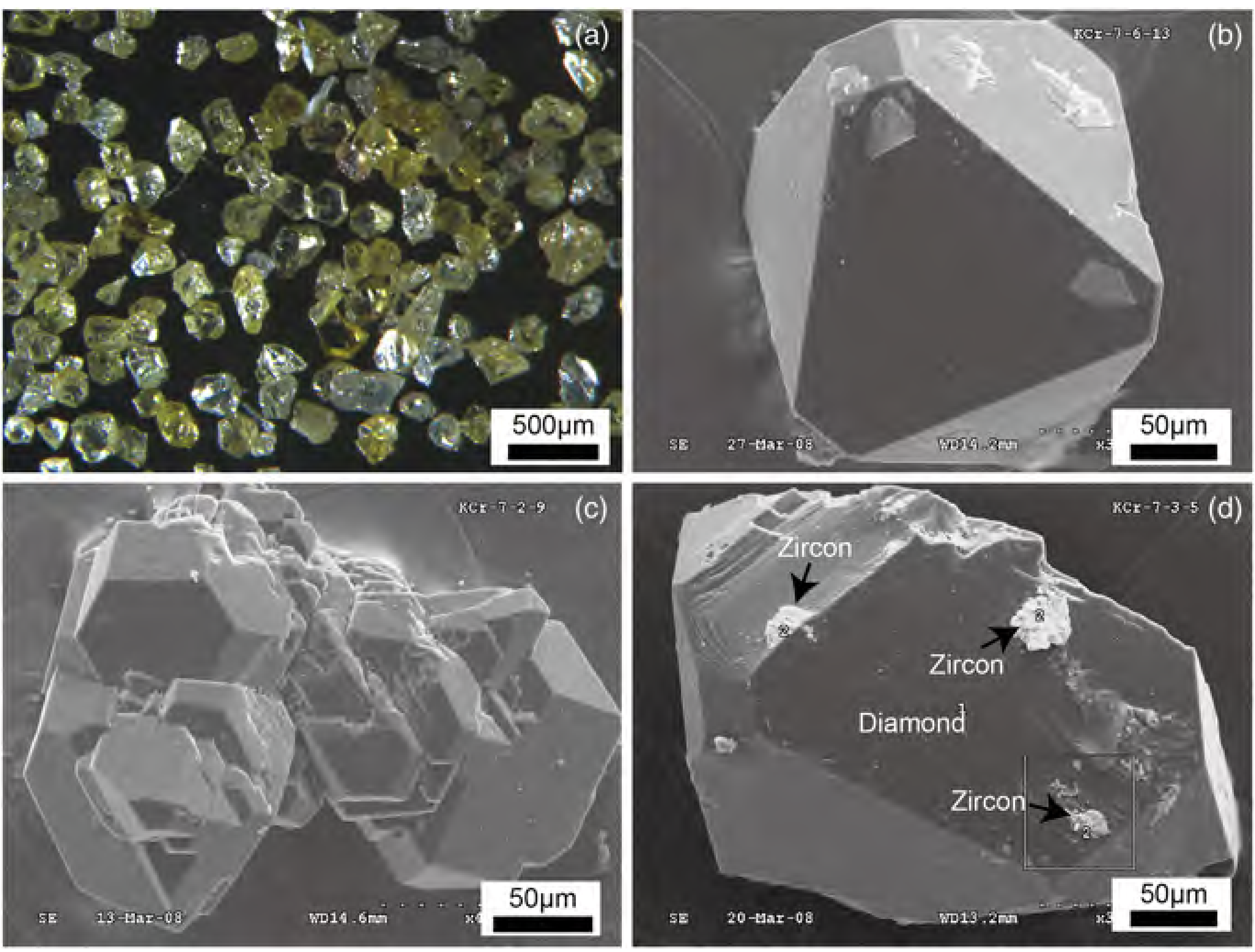

Fig. 7. Photographs of diamonds in Kangjinla chromitite. (a) Microphotograph showing abundant yellow and colorless diamonds; (b) SE image showing octahedral diamond; (c) SE image showing diamonds with polycrystalline; (d) SE image showing zircon attached to the surface of diamond.

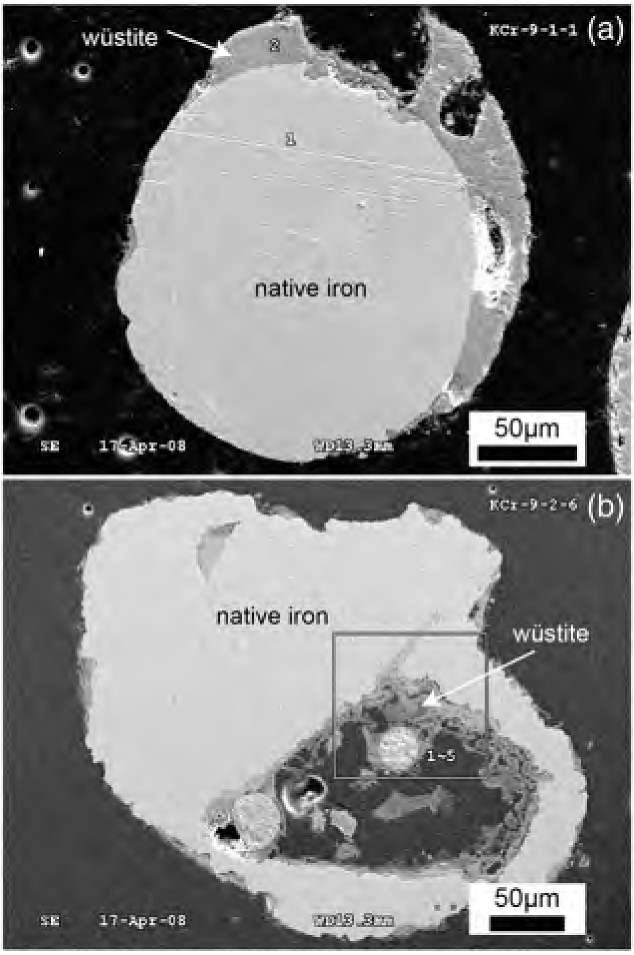

Fig. 8. Photographs showing the characteristics of native iron and wüstite in the Kangjinla chromitite. (a) SE image showing that wüstite (darker gray) forms rim on the native Fe (light gray); (b) SE image showing inclusions of wüstite (darker gray) in native iron (light gray).

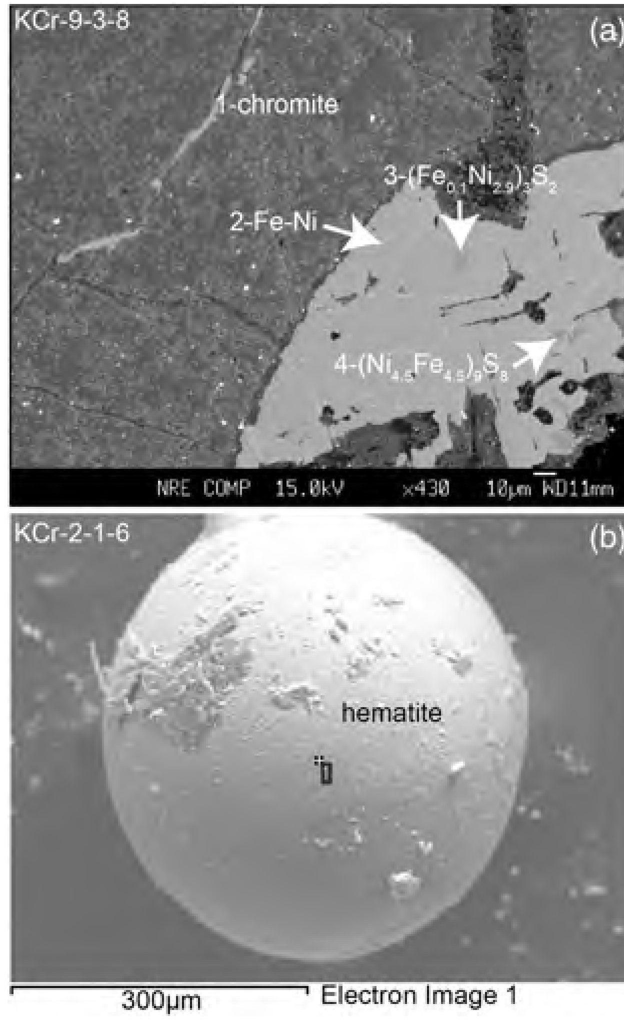

Fig. 9. Photographs of chromite with Fe–Ni alloy (a) and hematite (b) in the Kangjinla chromitite. (a) SE image showing chromite with Fe–Ni alloys, and droplet-shaped inclusions of Ni–Fe sulfides; (b) electron image of hematite showing the perfect spheres.

Thus, highly reduced elements and minerals are not likely to be preserved at the surface unless they were protected during passage through the oxidized layer. All shallow level processes that have operated in the ophiolite itself must have taken place under high oxygen fugacity, with the exception of minor serpentinization.

7.2. Comparison of UHP and highly reduced minerals from the Kangjinla chromitite and Ray-Iz chromitite of Russia

Over 60 mineral species, including diamond, moissanite, native elements and metal alloys have been separated from ~1500 kg of chromitite collected from two orebodies in the Ray-Iz ophiolite of the Polar Urals (Yang et al., 2014-in this issue). The Ray-Iz ophiolite consists mainly of lherzolite–harzburgite with minor dunite. The harzburgite is regarded as SSZ-type mantle peridotite, formed in a mantle wedge above a subduction zone (Perevozchikov et al., 2005; Shmelev, 2011). Unusual mineral groups from the Ray-Iz chromitite include: (1) native elements — Cr, W, Ni, Co, Si, Al and Ta; (2) carbides — SiC and WC; and (3) alloys — Cr–Fe, Si–Al–Fe, Ni–Cu, Ag–Au, Ag–Sn, Fe–Si, Fe–P, and Ag–Zn–Sn (Table 6). All of the minerals from the Ray-Iz chromitite are very similar to those reported from the Kangjinla chromitites, indicating that they are not restricted to one ophiolite or geographic region suggesting that they may be widespread in the oceanic mantle.

SEM images of diamonds (Fig. 11c, d) indicate that they have the same size (100–200 μm) and cubo-octahedra faces regardless of which ophiolite they occur in. Most of the diamonds 100–200 μm in diameter, but some in Tibet can exceed 500 μm. The diamonds are colorless and transparent, or yellowish-green. Many of the diamonds have euhedral forms (Figs. 7, 11), whereas others are broken or fractured. It is not clear whether the fracturing is a primary feature or it resulted from sample preparation.

Table 5
Representative X-ray diffraction data for Fe–Ni alloys in the Kangjinla chromitite.

D (Å)	I	D (Å)	I
(2.23)	3	1.252	8
20.4	10	(1.178)	2
(1.94)	2	(1.127)	1
1.770	5	1.070	10
(1.378)	2	1.024	4

Note: This is a polycrystalline alloy with a diffraction pattern similar to $Ni_{74}Fe_{25}$. The reference data are from the X-ray Mineral Powder Identification Manual edited by the Institute of Geochemistry, Chinese Academy of Sciences (card number 15).

7.3. Summary of mineral characteristics in the different ophiolites

Moissanite grains separated from the Kangjinla mantle peridotite and chromitite have similar shapes and colors and both contain traces of N. Moissanite recovered previously from orebody Cr 31 in Luobusa has an α-SiC structure (Bai et al., 2000) and the grains from Kangjinla are assumed to be the same. Experimental studies show that moissanite transforms into the β-SiC form at about 1500 °C and does not completely

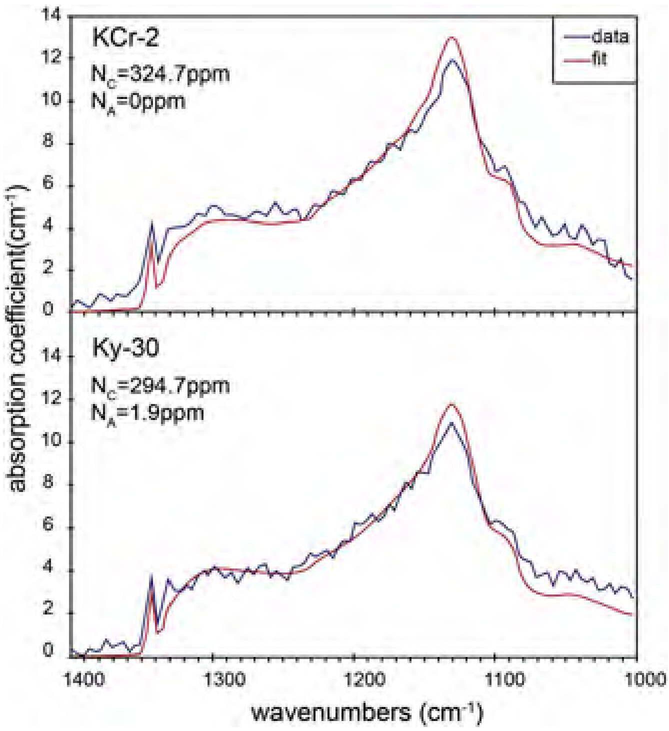

Fig. 10. Infrared absorption spectra of two microdiamonds from the chromitite (upper) and mantle peridotite (down) in Tibet.

transform into the α-SiC form until 2400 °C (Yajima et al., 1988). Thus, the presence of moissanite implies formation at both high temperature and high pressure. Some of the grains contain small inclusions of Fe–Si and native Si, indicating much reduced conditions of formation. The common occurrence of native Si, SiC and $FeSi_2$ in the chromitites requires fO_2 4 to 7 orders of magnitude below the IW buffer ($\Delta FMQ = -9$ to -12); the Si–SiO_2 buffer lies around $\Delta IW = -8$ (Trumbull et al., 2009; Shiryaev et al., 2011). Moissanite inclusions discovered in diamonds of the Rio São Luiz placer deposit are believed to have formed in the lower mantle (Wilding et al., 1991; Kaminsky, 2012). The high temperatures and highly reduced conditions needed for the formation of moissanite (Trumbull et al., 2009) similarly suggest a deep origin for the Kangjinla grains.

A striking feature of the chromitites and peridotites in Luobusa is the range and abundance of highly reduced phases, particularly native elements, metallic alloys and moissanite. Native elements and Fe–Ni alloys previously discovered in ophiolites have been interpreted either as primary grains (Melcher et al., 1997; Bai et al., 2000), or as secondary phases formed during serpentinization (Jamieson, 1905; Dick, 1974). Bird and Weathers (1975) stressed that Fe–Ni alloys commonly contain inclusions of native silicon and hence are thought to have formed at high temperatures and high pressures. Although serpentinization can produce such grains (Fig. 6) (Dick, 1974), Fe–Ni alloys are commonly associated with PGE minerals in many chromitites that show little serpentinization (e.g. Bai et al., 2000; Ahmed and Arai, 2002; Bai et al., 2004). In addition, the association of native iron + wüstite has been found as inclusions in diamonds of the Koryak peridotite (Rudashevsky et al., 1987) and in a kimberlite in Tanzania. The kimberlite assemblage was interpreted as being from the lower mantle, perhaps from depths > 670 km (Stachel et al., 1998). Kaminsky (2012) suggested that the mineral associations (wüstite + periclase and native iron + iron carbide) may be related to the D′ layer at the core/mantle boundary. Thus, we agree with Bai et al. (2006a, 2007) that these phases came from the deep upper mantle or the lower mantle.

The small spheres of native iron are similar in size and morphology to I-type spherules which have been described from young sediments (Taylor et al., 1996; Stankowski et al., 2006), and which are typically assumed to be cosmic in origin. However, such grains have been found in chromitites of the Luobusa ophiolite (Bai et al., 2000; Robinson et al., 2014-in this issue), the Ray-Iz ophiolite in Russia (Yang et al., 2014-in this issue) and the Semail ophiolite of Oman (Robinson et al., 2014-in this issue), where they are associated with the other highly reduced phases that had a mantle origin. Thus, we believe that spherules of native iron are indigenous to the chromitites and, like the related elements and alloys, had a deep mantle origin.

The stability of metal phases is controlled mostly by fO_2 (Ballhaus, 1995), and native Fe is possibly stable at depths greater than 250 km (Rohrbach et al., 2007). Native Fe can stably coexist with olivine (Fo_{90}) and orthopyroxene at very low fO_2 (Ballhaus, 1995). Metallic Fe can exist at far more reduced conditions (Wood et al., 1990; Ballhaus et al., 1991). The alloys in the Kangjinla chromitite and mantle peridotite are primarily Fe–Ni alloys with Ni/Fe ratios of about 7/3–8/2, making them similar to Fe–Ni alloys reported previously from orebody 31 of Luobusa (Bai et al., 2000). Most of the other alloys from Kangjinla occur as inclusions in grains of corundum. Interestingly, most of the Fe–Ni alloys in the chromitite contain numerous inclusions, such as Ni-bearing pyrite, Fe-bearing periclase and magnesium silicate, all of which are absent in the alloys from the peridotite.

7.4. Origin of the peridotites and chromitites of the Luobusa ophiolite

Diamonds, moissanite and highly reduced minerals have been found for the first time in Kangjinla chromitite orebody Cr-11 (Fig. 7), and these phases are much more abundant than similar minerals in the Luobusa ophiolite (e.g. orebody 31 and the Luobusa district), even though they are only about 20 km apart. We also demonstrated that many of these minerals occur in the host peridotites, as well as in the chromitites. Thus, this work not only confirmed the existence of special mantle minerals in the ophiolite but expanded our understanding of their distribution and occurrence, providing new insight into the nature of deep mantle minerals in ophiolites.

The mantle peridotites are typical residues of partial melting and melt/rock reaction, consisting essentially of olivine and orthopyroxene, with minor clinopyroxene and magnesiochromite. The wide range of unusual minerals in the chromitites and peridotites clearly indicates formation in a variety of temperatures, pressures and oxygen fugacities. So the origin of the ophiolites and chromitites must be more complicated than previously thought.

Based on many studies of ophiolites, it is generally accepted that ophiolites and podiform chromitites form at shallow mantle levels in suprasubduction zone environments (Arai and Yurimoto, 1994; Zhou et al., 1994, 1996; Edwards et al., 2000; Rollinson and Adetunji, 2013b).

Table 6
UHP and highly reduced minerals recovered from the mantle peridotites and chromitites in the Tibetan and Ray-Iz ophiolites.

	Mantle peridotite (Kangjinla)	Chromitite (Kangjinla)	Mantle peridotite (Purang)	Chromitite (Ray-Iz)
UHP mineral	Diamond	Diamond	Diamond	Diamond
Highly reduced mineral	Moissanite, Fe, Fe–Ni, Ni–Mn–Co, Fe–Cr–Ni	Moissanite, Fe, Ta, Fe–Ni–Cr, Mn–Ni, Fe–Si, P–Si–Ti, Ti–Si, Co–Mn–Ni, Ti–N, Ti–C, Ti–B	Moissanite, Fe, Cr, Zn, Fe–Ni, Fe–Cr	Cr, W, Ni, Co, Si, Al, Ta, WC, SiC, Os–Ir–Ru, Cr–Fe, Si–Al–Fe, Ni–Cu, Ag–Au, Ag–Sn, Fe–Si, Fe–P, and Ag–Zn–Sn

Note: the data from the Purang referred to the Yang et al. (2011); the data from the Ray-Iz referred to the Yang et al. (2014-in this issue).

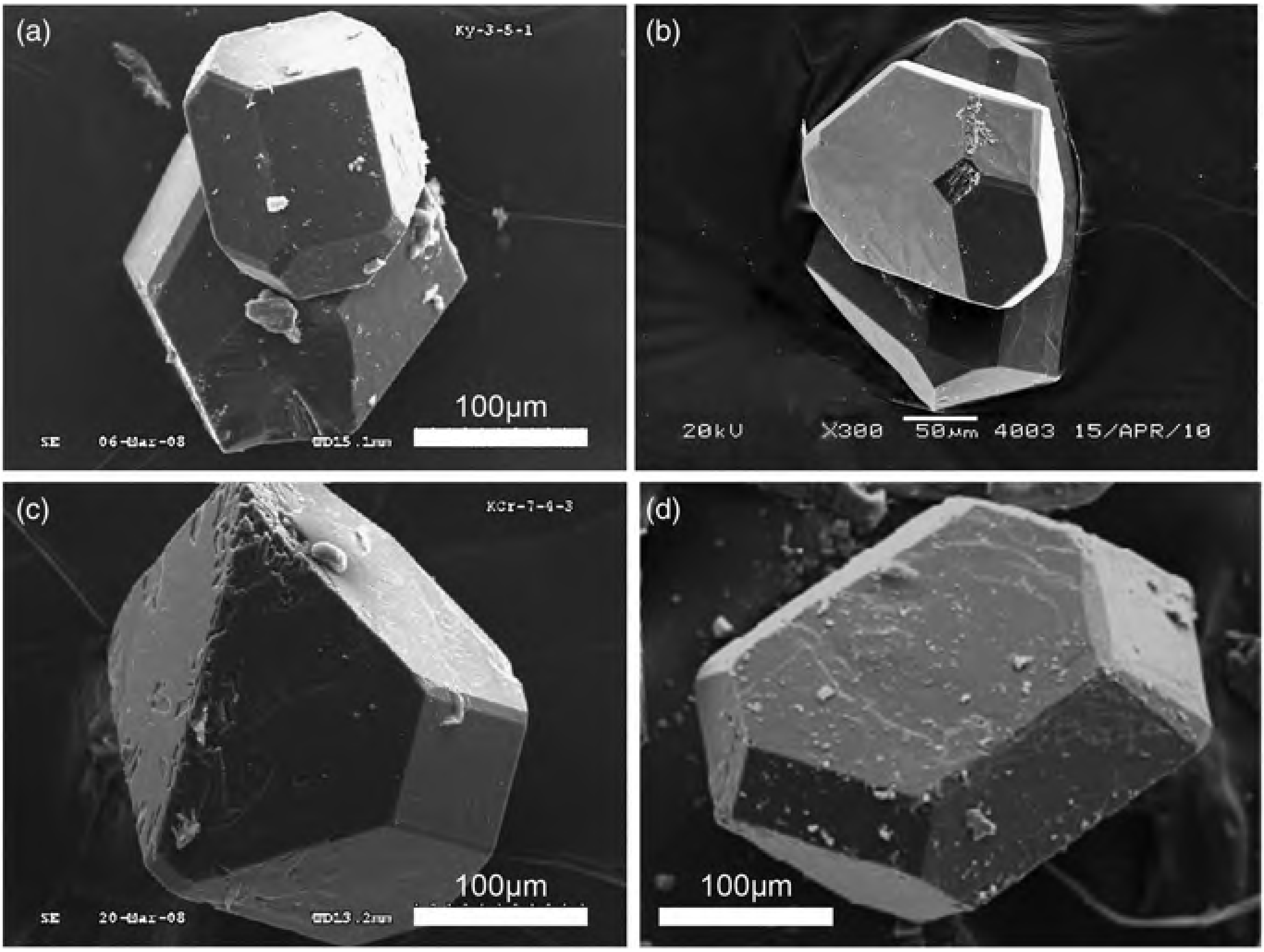

Fig. 11. SE image of diamond from the chromitite and peridotites in the Tibet and Ray-Iz. (a) SE image of diamond from the Kangjinla mantle peridotite; (b) SE image of diamond from the Purang mantle peridotite; (c) SE image of diamond from the Kangjinla chromitite; (d) SE image of diamond from the Ray-Iz chromitite.

Clearly, the presence of UHP and highly reduced minerals in the Luobusa ophiolite is not easily reconciled with this model. On the basis of two small (2–3 cm) micropods of chromitite recovered from in-situ oceanic lithosphere, Arai et al. (1997) suggested that chromitites form beneath mid-ocean spreading ridges, as well as in SSZ environments. Such a model might explain the presence of the UHP and highly reduced minerals in chromitites, but it does not explain how the chromitites were able to rise from great depth and be emplaced in the uppermost levels of the Luobusa ophiolite, which formed in a suprasubduction zone environment. Nor does it explain how the UHP and highly reduced minerals were preserved in the peridotites as well as the chromitites. The in-situ occurrence of diamonds and moissanite leaves no doubt that these minerals are intrinsic to the ophiolite (Yang et al., 2014). Dating of zircons show that many of the crustal-type minerals are older than the ophiolite, suggesting that these minerals are remnants of partially digested oceanic crust and sediments carried into the mantle by subduction (Robinson et al., 2014-in this issue; Yamamoto et al., 2013). The ancient crustal zircons discovered from in the Luobusa chromitites are key evidence of mantle inhomogeneity and recycling of crust materials. Considering the coexistence of unusual mantle minerals and possible cyclic crustal materials, the origin of the Luobusa chromitite might bear certain relationship with mantle plume (Fig. 12; Xiong et al., 2014; Yang et al., 2014).

We suggest that microdiamonds may be widely present in the upper oceanic mantle below about 150 km. Several lines of evidence suggest that chromite crystallization can take place anywhere in the mantle above about 380 km (Yamamoto et al., 2009). The coesite grains rimming with a Fe–Ti alloy from a Luobusa is probably pseudomorphic after stishovite, implying a pressure of formation over 9 GPa, roughly 300 km depth (Yang et al., 2007a). This interpretation is supported by nano-scale inclusions of TiN, cubic BN, native Fe and TiO_2 in the coesite, indicating a minimum pressure of 10 GPa (Dobrzhinetskaya et al., 2009). Similar inclusions such as TiN and TiO_2 occur in corundum grains from Kangjinla, suggesting crystallization at depth (Xu et al., 2013).

Some of the UHP minerals found in podiform chromitites are C-bearing, suggesting their possible importance in the deep carbon cycle (Arai, 2010). Arai (2010, 2013) proposed deep recycling of the chromitites containing UHP, suggesting that they formed originally at shallow levels in the upper mantle before sinking down to deeper mantle and upwelling again to the uppermost mantle by convection. However, this model does not explain how the UHP minerals become entrained in the chromitites during recycling. It is also difficult to reconcile with the lack of any known significant bodies of chromitite in in-situ oceanic mantle and the clear evidence for chromite crystallization and accumulation in SSZ environments.

Thus, we propose that individual chromite grains crystallizing at depth encapsulated the diamonds and highly reduced phases described in this paper. Such grains which are normal parts of the oceanic mantle rise upward during mantle convection. Some segments of such mantle become trapped in SSZ environments where they are modified by hydrous melts and fluids. The chromite grains are re-mobilized in such

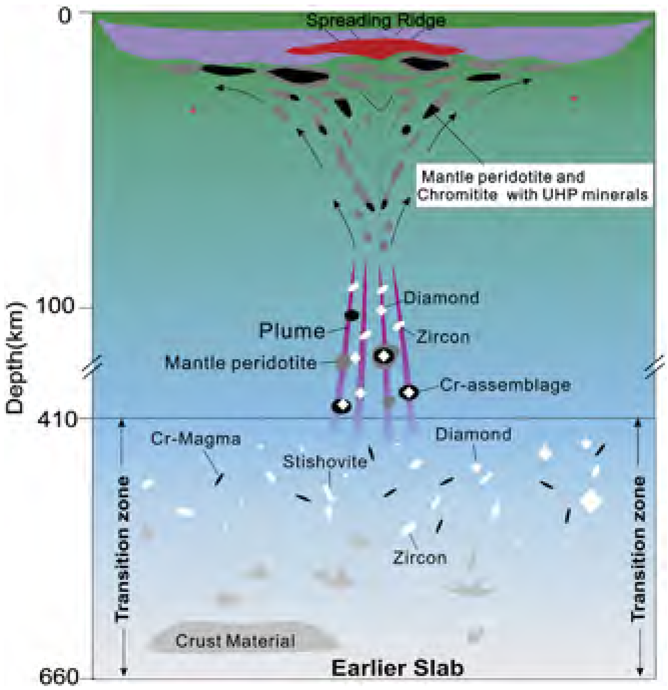

Fig. 12. Cartoon figure of formation of the mantle peridotite and chromitite containing the ultrahigh-pressure minerals.
Revised after Xiong et al. (2014) and Yang et al. (2014).

environments, modified by melt/rock reaction and redeposited to form podiform bodies. The UHP and highly reduced minerals are preserved in these grains because they are encased in chromite. Theory (Smyth, 1987) and experiments (Kohlstedt et al., 1996; Chen et al., 2002; Bercovici and Karato, 2003) have shown that although the water storage capacity of olivine-dominated, shallow mantle is limited, but water is thought to exist in the Earth's transition zone, at depths between 410 and 660 km. The ultimate origin of water in the Earth's hydrosphere is considered to be from the deep mantle. An inclusion of ringwoodite containing a small amount of water in a deep diamond lends support to this view (Pearson et al., 2014). So, enriched carbon fluids and earlier slab materials exist in the transition zone, and may be source for the diamonds and moissanite. In addition, fluids released from subducted oceanic and continental crust metasomatize the depleted peridotites in the SSZ mantle wedges, leading to formation of hydrous, high-Mg, high-Si melts. These migrating melts mobilized chromite grains and increase their Cr# by melt–rock reaction. Clearly, the available evidence points to complex, multi-stage process for the formation of ophiolites and their podiform chromitites.

Since this study was completed, we have sampled peridotites in all of the major ophiolitic blocks in the Yarlung-Zangbo suture zone, which include from east to west, the Luobusa, Zedang, Xigaze, Dangqiong, Purang, and Dongbo massifs. A similar collection of UHP and highly reduced phases has been recovered from all of these bodies, indicating that these minerals are widespread (Xu et al., 2011a; Yang et al., 2011). Similar minerals have also been recovered from the Ray-Iz ophiolite of the Polar Urals (Yang et al., 2007b, 2014-in this issue). The nature of the ophiolite-hosted diamonds and their inclusions, as well as their occurrence in oceanic mantle rocks, indicate that they represent a new type of diamond occurrence, completely different from that of kimberlites and UHP metamorphic belts (Yang et al., 2014).

8. Conclusions

Although much work remains before we can clearly understand the formation and evolution of ophiolites, any model needs to explain the presence of UHP minerals and highly reduced minerals in both the chromitites and peridotites. UHP minerals may be a normal part of the mantle peridotite and chromitite, not only in Yarlung Zangbo suture zone, but also in other ophiolites and chromitites. We suggest a plausible model that brings together these different elements in the mantle transition zone. Subduction of oceanic and continental lithospheric slabs introduces crustal minerals into the upper mantle, where they are mixed with highly reduced phases brought from the lower mantle simple convection (Fig. 12). Crystallizing chromite grains above the transition zone encapsulate these minerals and protect them from further modification. Mantle convection, either beneath mid-ocean spreading centers or back-arc basins, carries the resulting peridotites and chromite grains to shallow levels. Most of the lithospheric slabs formed at spreading ridges are recycled into the mantle by subduction but some mantle wedges are trapped above subduction zones where they are modified by SSZ melts and fluids. We believe that the available evidence strongly supports a model involving formation of podiform chromitites within such SSZ environments.

Acknowledgments

This research was funded by grants from Sinoprobe-05-02 of the Ministry of Science and Technology of China (SinoProbe-05-02), the NSF China (Nos. 41202036, 40930313, 40921001), and the China Geological Survey (No. 12120114061801). We are very grateful to Professor Mei-Fu Zhou and Dr. Shinji Yamamoto for their constructive reviews of the manuscript. We thank Yan Ling and Chen Fangyuan of the State Key Laboratory of Continental Tectonic and Dynamic for their assistance with sample preparation, as well as laser Raman and compositional analyses. Tao Shufeng of the Beijing General Research Institute of Mining and Metallurgy is thanked for his assistance with the compositional analyses, and Liu Chengdong of State Key Laboratory Breeding Base of Nuclear Resources and Environment, East China Institute of Technology is thanked for his assistance with the electron probe microanalyses.

References

Ahmed, A.H., Arai, S., 2002. Unexpectedly high-PGE chromitite from the deeper mantle section of the northern Oman ophiolite and its tectonic implications. Contributions to Mineralogy and Petrology 143, 263–278.

Arai, S., 2010. Possible recycled origin for ultrahigh-pressure chromitites in ophiolites. Journal of Mineralogical and Petrological Sciences 105, 280–285.

Arai, S., 2013. Conversion of low-pressure chromitites to ultrahigh-pressure chromitites by deep recycling: a good inference. Earth and Planetary Science Letters 379, 81–87.

Arai, S., Yurimoto, H., 1994. Podiform chromitites of the Tari-Misakaultra mafic complex, southwestern Japan, as mantle–melt interaction products. Economic Geology 89, 1279–1288.

Arai, S., Matsukage, K., Isobe, E., Vysotskiy, S., 1997. Concentration of incompatible elements in oceanic mantle: effect of melt/wall interaction in stagnant or failed melt conduits within peridotite. Geochimica et Cosmochimica Acta 61, 671–675.

Bai, W.J., Zhou, M.F., Robinson, P.J., 1993. Possibly diamond-bearing mantle peridotites and podiform chromitites in the Luobusa and Dongqiao ophiolites, Tibet. Canadian Journal of Earth Sciences 30, 1650–1659.

Bai, W.J., Zhou, M.F., Robinson, P.T., Fang, Q.S., Zhang, Z.M., Yan, B.G., Hu, X.F., Yang, J.S., 2000. Origin of Podiform Chromitites, Diamond and Associated Mineral Assemblages in the Luobusa Ophiolite, Tibet. Seismological Press, Beijing (in Chinese with English abstract).

Bai, W.J., Yang, J.S., Robinson, P., Fang, Q.S., Zhang, Z.M., Yan, G.G., Hu, X.F., 2001. Study of diamonds from chromitites in the Luobusa ophiolite, Tibet. Acta Geologica Sinica 75, 404–409 (in Chinese with English abstract).

Bai, W.J., Robinson, P.T., Fang, Q.S., Yang, J.S., Yan, B.G., Zhang, Z.M., Hu, X.F., Zhou, M.F., 2004. The PGE and base-metal alloys in the podiform chromitites of the Luobusa Ophiolite, Southern Tibet. Acta Geoscientia Sinica 25 (4), 385–396 (in Chinese with English abstract).

Bai, W.J., Ren, Y.F., Yang, J.S., Fang, Q.S., Yan, B.G., Rong, H., 2006a. The native iron and wustite assemblage: records of oxygen element from the mantle. Acta Geoscientia Sinica 27 (1), 43–49 (in Chinese with English abstract).

Bai, W.J., Shi, N.C., Fang, Q.S., Li, G.W., Xiong, M., Yang, J.S., Rong, H., 2006b. Luobusaite: a new mineral. Acta Geologica Sinica 80, 656–659.

Bai, W.J., Shi, N.C., Yang, J.S., Fang, Q.S., Ren, Y.F., Rong, H., Li, G.W., Ma, Z.S., 2007. An assemblage of simple oxide minerals from ophiolitic podiform chromitites in Tibet and their ultrahigh pressure origin. Acta Geologica Sinica 81 (11), 1538–1549 (in Chinese with English abstract).

Ballhaus, C., 1995. Is the upper mantle metal-saturated? Earth and Planetary Science Letters 132, 75–86.

Ballhaus, C., Berry, R.F., Green, D.H., 1991. High pressure experimental calibration of the olivine–orthopyroxene–spinel oxygen geobarometer: implications for the oxidation state of the upper mantle. Contributions to Mineralogy and Petrology 107, 27–40.

Bercovici, D., Karato, S., 2003. Whole-mantle convection and the transition zone water filter. Nature 425, 39–44.

Bird, J.M., Weathers, M.S., 1975. Josephinite: specimens from the Earth's core? Earth and Planetary Science Letters 28, 51–64.

Boyd, S.R., Kiflawi, I., Woods, G.S., 1994. The relationship between infrared absorption and the A defect concentration in diamond. Philosophical Magazine Part B 69, 1149–1153.

Boyd, S.R., KIflawi, I., Woods, G.S., 1995a. Infrared absorption by the B nitrogen aggregate in diamond. Philosophical Magazine Part B 72, 351–361.

Boyd, S.R., Réjou-Michel, A., Javory, M., 1995b. Improved techniques for the extraction, purification and quantification of nanomole quantities of nitrogen gas: the nitrogen content of a diamond. Measurement Science and Technology 6, 297–305.

Cartigny, P., Boyd, S., Harris, J., Javoy, M., 1997. Nitrogen isotopes in peridotitic diamonds from Fuxian, China: the mantle signature. Terra Nova 9 (4), 175–179.

Cartigny, P., de Corte, K., Shatsky, V.S., Ader, M., de Paepe, P., Sobolev, N.V., Javoy, M., 2001. The origin and formation of metamorphic microdiamonds from the Kokchetav massif, Kazakhstan: a nitrogen and carbon isotopic study. Chemical Geology 176, 265–281.

Cartigny, P., Harris, J.W., Taylor, A., Davies, R., Javoy, M., 2003. On the possibility of a kinetic fractionation of nitrogen stable isotopes during natural diamond growth. Geochimica et Cosmochimica Acta 67 (8), 1571–1576.

Chen, J., Inoue, T., Yurimoto, H., Weidner, D.J., 2002. Effect of water on olivine–wadsleyite phase boundary in the (Mg, Fe)$_2$SiO$_4$ system. Geophysical Research Letters 29, 22-1–22-4.

Chrenko, R.M., Tuft, R.E., Strong, H.M., 1977. Transformation of the state of nitrogen in diamond. Nature 270, 141–144.

Dick, H.J.B., 1974. Terrestrial nickel–iron from the josephinite peridotite, its geologic occurrence, associations and origin. Earth and Planetary Science Letters 24, 291–298.

Dick, H.J.B., Bullen, T., 1984. Chromium spinel as a petrogenetic indicator in abyssal and alpine-type peridotites and spatially associated lavas. Contributions to Mineralogy and Petrology 86 (1), 54–76.

Dobretsov, N.L., Sobolev, N.V., Shatsky, V.S., Goleman, R.G., Ernst, W.G., 1995. Geotectonic evolution of diamondiferous paragneisses, Kokchetav complex, northern Kazakhstan: the geologic enigma of ultrahigh-pressure crustal rocks within a Paleozoic foldbelt. Island Arc 4, 267–279.

Dobrzhinetskaya, L.F., 2012. Microdiamonds — frontier of ultrahigh-pressure metamorphism: a review. Gondwana Research 21, 207–223.

Dobrzhinetskaya, L.F., Liu, Z., Cartigny, P., Zhang, J., Tchkhetia, N.N., Green II, H.W., Hemley, R.J., 2006. Synchrotron infrared and Raman spectroscopy of microdiamonds from Erzgebirge, Germany. Earth and Planetary Science Letters 248, 340–349.

Dobrzhinetskaya, L.F., Wirth, R., Yang, J.S., Hutcheon, I.D., Weber, P.K., Green, H.W.II, 2009. High-pressure highly reduced nitrides and oxides from chromitite of a Tibetan ophiolite. PNAS Early Edition pp. 1–6.

Edwards, S.J., Pearce, J.A., Freeman, J., 2000. New insights concerning the influence of water during the formation of podiform chromitite. In: Dilek, Y., Moores, E.M., Elthon, D., Nicolas, A. (Eds.), Ophiolites and Oceanic Crust: New Insights From Field Studies and the Ocean Drilling Program. Geological Society of America Special Paper, 349, pp. 139–147.

Fang, Q.S., Bai, W.J., Yang, J.S., Xu, X.Z., Li, G.W., Shi, N.C., Xiong, M., Rong, H., 2009. Qusongite (WC): a new mineral. American Mineralogist 94, 387–390.

Field, M., Stiefenhofer, J., Bobey, J., Kurszlaukis, S., 2008. Kimberlite-hosted diamond deposits of southern Africa: a review. Ore Geology Reviews 34, 33–75.

Finnie, K.S., Fisher, D., Griffin, W.L., Harris, J.W., Sobolev, N.V., 1994. Nitrogen aggregation in metamorphic diamonds from Kazakhstan. Geochimica et Cosmochimica Acta 58, 5173–5177.

Frost, D.J., Liebske, C., Langenhorst, F., McCammon, C.A., Trфnnes, R.G., Rubie, D.C., 2004. Experimental evidence for the existence of iron-rich metal in the Earth's lower mantle. Nature 428, 409–412.

Griffiin, W., Yang, J., Robinson, P.T., Howell, D., Shi, R.D., O'Reilly, S., Pearson, N., 2013. Going up or going down? Diamonds and super-reducing UHP assemblages in ophiolitic mantle. Mineralogical Magazine 77 (5), 1215.

Hu, X.F., 1999. Origin of Diamonds in Chromitites of the Luobusa Ophiolite, Southern Tibet, ChinaMSc Thesis Dalhousie University, Halifax, Nova Scotia, Canada, p. 151.

Institute of Geology, Chinese Academy of Geological Sciences, 1981. The discovery of alpine-type diamond bearing ultrabasic intrusions in Xizang (Tibet). Geological Review 27 (5), 445–447 (in Chinese).

Jamieson, G.S., 1905. On the natural iron–nickel alloy awaruite. American Journal of Science 19, 413–415.

Kaminsky, F., 2012. Mineralogy of the lower mantle: a review of 'super-deep' mineral inclusions in diamond. Earth-Science Reviews 110, 127–147.

Kohlstedt, D.L., Keppler, H., Rubie, D.C., 1996. Solubility of water in the α, β and γ phases of (Mg, Fe)$_2$SiO$_4$. Contributions to Mineralogy and Petrology 123, 345–357.

Li, G.W., Fang, Q.S., Shi, N.C., Bai, W.J., Yang, J.S., Xiong, M., Ma, Z.S., Rong, H., 2010. A new natural Ti–Fe–Si alloy mineral: zangboite. Acta Mineralogica Sinica S1, 7–8 (in Chinese).

MacLeod, C.J., Lissenberg, C.J., Bibby, L.E., 2013. 'MoistMORB' axial magmatism in the Oman ophiolite: the evidence against a mid ocean ridge origin. Geology 41, 459–462. http://dx.doi.org/10.1130/G33904.1.

McCammon, C.A., 2005. The paradox of mantle redox. Science 308, 807–808.

Melcher, F., Grum, W., Simon, G., Thalhammer, T.V., Stumpfl, E.F., 1997. Petrogenesis of giant chromite deposits of Kempirsai, Kazakhstan: a study of solid and fluid inclusions in chromite. Journal of Petrology 38, 1419–1458.

Ogasawara, Y., 2005. Microdiamonds in ultrahigh-pressure metamorphic rocks. Elements 1, 91–96.

Pearson, D.G., Brenker, F.E., Nestola, F., McNeill, J., Nasdala, L., Hutchison, M.T., Matveev, S., Mather, K., Silversmit, G., Schmitz, S., Vekemans, B., Vincze, L., 2014. Hydrous mantle transition zone indicated by ringwoodite included within diamond. Nature 507, 221–224.

Perevozchikov, B.V., Kenig, V.V., Lukin, A.A., Ovechkin, A.M., 2005. Chromites of the Rai-Iz massif in the Polar Urals (Russia). Geology of Ore Deposits 47, 206.

Richardson, S.H., Gurney, J.J., Erlank, A.J., Harris, J., 1984. Origin of diamonds in old enriched mantle. Nature 310, 198–202.

Robinson, P.T., Bai, W.J., Malpas, J., Yang, J.S., Zhou, M.F., Fang, Q.S., Hu, X.F., Cameron, S., Staudigel, H., 2004. Ultra-high pressure minerals in the Luobusa ophiolite, Tibet and their tectonic implications. Aspects of the tectonic evolution of China. Geological Society, London, Special Publications 226, 247–271.

Robinson, P.T., Trumbull, R.B., Schmitt, A., Yang, J.S., Li, J.W., Zhou, M.F., Erzinger, J., Xiong, F.H., 2014. The origin and significance of crustal minerals in ophiolitic chromitites and peridotites. Gondwana Research 27, 486–506 (in this issue).

Rohrbach, A., Balhaus, C., Golla-Schindler, U., Ulmer, P., Kamenetsky, V.S., Kuzmin, D.V., 2007. Metal saturation in the upper mantle. Nature 449, 456–458.

Rollinson, H., Adetunji, J., 2013a. Mantle podiform chromitites do not form beneath mid-ocean ridges: a case study from the Moho transition zone of the Oman ophiolite. Lithos 177, 314–327.

Rollinson, H., Adetunji, J., 2014b. The geochemistry and oxidation state of podiform chromitites from the mantle section of the Oman ophiolite: a review. Gondwana Research 27, 543–554.

Rong, H., Yang, J.S., Zhang, Z.M., Xu, X.Z., 2013. A preliminary study of FT-IR on the diamonds from the Luobusa chromitites of Tibet and the eclogite of CCSD-MH, China. Acta Petrologica Sinica 29, 1861–1866 (in Chinese with English abstract).

Rudashevsky, N.S., Dmitrenko, G.G., Mochalov, A.G., 1987. Native metals and carbides in Alpine type ultramafics of Koryak Highland. Mineralogicheskii Zhurnal 9 (4), 71–82 (in Russian).

Shi, N.C., Bai, W.J., Li, G.W., Xiong, M., Fang, Q.S., Yang, J.S., Ma, Z.S., Rong, H., 2009. Yarlongite: a new metallic carbide mineral. Acta Geologica Sinica 83 (1), 25–30 (in Chinese with English abstract).

Shiryaev, A.A., Griffin, W.L., Stovanov, E., 2011. Moissanite (SiC) from kimberlites: polytypes, trace elements, inclusions and speculations on origin. Lithos 122, 152–164.

Shmelev, V.R., 2011. Mantle ultrabasites of ophiolite complexes in the Polar Urals: petrogenesis and geodynamic environments. Petrology 19, 618–640.

Smyth, J.R., 1987. β-Mg$_2$SiO$_4$: a potential host for water in the mantle? American Mineralogist 72, 1051–1055.

Stachel, T., Harris, J.W., Brey, G.P., 1998. Pare and unusual mineral inclusions in diamonds from Mwadui, Tanzania. Contributions to Mineralogy and Petrology 132, 34–47.

Stankowski, W.T.J., Katrusiak, J.A., Budzianowaki, A., 2006. Crystallographic variety of magnetic spherules from Pleistocene and Holocene sediments in the Northern foreland of Morasko-Meteorite Reserve. Planetary and Space Science 54, 60–70.

Taylor, W.R., Jaques, A.L., Ridd, M., 1990. Nitrogen-defect aggregation characteristics of some Australasian diamonds: time–temperature constraints on the source regions of pipe and alluvial diamonds. American Mineralogist 75, 1290–1310.

Taylor, W.R., Milledge, H.J., Griffin, B.J., Nixon, P.H., Kamperman, M., Mattey, D.P., 1995. Characteristics of microdiamonds from ultramafic massifs in Tibet: authentic ophiolitic diamonds or contamination? 6th International Kimberlite Conference Extended Abstract, Russia, Novosibirsk, pp. 623–624.

Taylor, P.L., Nusbaum, R.L., Fronabarger, A.K., Katuna, M.P., Summer, N., 1996. Magnetic spherules in coastal plain sediments, Sullivan's Island, South Carolina, USA. Magnetic spherules in coastal plain sediments, Sullivan's Island, South Carolina, USA. Meteoritics & Planetary Science 31, 77–80.

Trumbull, R.B., Yang, J.S., Robinson, P.T., Pierro, S.D., Vennemann, T., Wiedenbeck, M., 2009. The carbon isotope composition of natural SiC (moissanite) from the Earth's mantle: new discoveries from ophiolites. Lithos 113, 612–620.

Wang, H.S., Bai, W.J., Wang, B.X., Cai, Y.C., 1983. Chromite Deposits in China and Their Origin. Science Press, Beijing, pp. 1–227 (in Chinese).

Wang, X.B., Bao, P.S., Deng, W.M., Wang, F.G., 1987. Tibet Ophiolites. Geological Publishing House, Beijing, pp. 1–336 (in Chinese).

Wilding, M.C., Harte, B., Harris, J.W., 1991. Evidence for a deep origin for the Sao Luiz diamonds. Fifth International Kimberlite Conference Extended Abstracts, Araxa, pp. 456–458.

Wood, B.J., Bryndzia, L.T., Johnson, K.E., 1990. Mantle oxidation state and its relationship to tectonic environment and fluid speciation. Science 248, 337–345.

Xiong, F.H., Yang, J.S., Liu, Z., Guo, G.L., Chen, S.Y., Xu, X.Z., Li, Y., Liu, F., 2013. High-Cr and high-Al chromitite found in western Yaulung-Zangbo suture zone in Tibet. Acta Petrologica Sinica 29 (6), 1878–1908 (in Chinese with English abstract).

Xiong, F.H., Yang, J.S., Robinson, P.T., Xu, X.Z., Liu, Z., Li, Y., Liu, F., Chen, S.Y., 2014. Origin of podiform chromitite, a new model based on the Luobusa ophiolite, Tibet. Gondwana Research 27, 525–542.

Xu, X.Z., 2009. Origin of the Kangjinla podiform chromite deposit and mantle peridotite, South Tibet. Beijing: A Dissertation Submitted to Chinese Academy of Geological Science for Doctoral Degree, p. 145 (in Chinese with English abstract).

Xu, X.Z., Yang, J.S., Ba, D.Z., Chen, S.Y., Fang, Q.S., Bai, W.J., 2008. Diamond discovered from the Kangjinla chromitite in the Yarlung Zangbo ophiolite belt, Tibet. Acta Petrologica Sinica 24 (7), 1453–1462 (in Chinese with English abstract).

Xu, X.Z., Yang, J.S., Chen, S.Y., Fang, Q.S., Bai, W.J., Ba, D.Z., 2009. An unusual mantle mineral group from chromitite orebody Cr-11 in the Luobusa ophiolite of the Yarlung-Zangbo suture zone, Tibet. Journal of Earth Science 20 (2), 284–302.

Xu, X.Z., Yang, J.S., Ba, D., Li, Y., Liu, Z., 2011a. Diamonds discovered in five peridotite massifs along the Yarlung-Zangbo suture in South Tibet: tectonic implications. 2011 AGU Fall Meeting V11H-06.

Xu, X.Z., Yang, J.S., Ba, D.Z., Guo, G.L., Robinson, P.T., Li, J.Y., 2011b. Petrogenesis of the Kangjinla peridotite in the Luobusa ophiolite, Southern Tibet. Journal of Asian Earth Sciences 42, 553–568.

Xu, X.Z., Yang, J.S., Guo, G.L., Xiong, F.H., 2013. Mineral inclusions in corundum from chromitites in the Kangjinla chromite deposit, Tibet. Acta Petrologica Sinica 29 (6), 1867–1877 (in Chinese with English abstract).
Yajima, L., Doi, M., Kurumoto, 1988. Sinterability of submicron B-SiC powder synthesized by carbothermal reduction of silica. Silicon Carbide Ceramics 2, 39–49.
Yamamoto, S., Komiya, T., Hirose, K., Maruyama, S., 2009. Coesite and clinopyroxene exsolution lamellae in chromites: in-situ ultrahigh-pressure evidence from podiform chromitites in the Luobusa ophiolite, southern Tibet. Lithos 109, 314–322.
Yamamoto, S., Komiya, T., Yamamoto, H., Kaneko, Y., Terabayashi, M., Katayama, I., Iizuka, T., Maruyama, S., Yang, J., Kon, Y., Hirata, T., 2013. Recycled crustal zircons from podiform chromitites in the Luobusa ophiolite, southern Tibet. Island Arc 22, 9–103.
Yang, J.S., Bai, W.J., Fang, Q.S., Yan, B.G., Shi, N.C., Ma, Z.S., Dai, M.Q., Xiong, M., 2003. Silicon-rutile — an ultrahigh pressure (UHP) mineral from an ophiolite. Progress in Natural Science 13 (7), 528–531.
Yang, J.S., Dobrzhinetskaya, L., Bai, W.J., Fang, Q.S., Robinson, P.T., Zhang, J.F., Green, H.W. II., 2007a. Diamond- and coesite-bearing chromitites from the Luobusa ophiolite, Tibet. Geology 35 (10), 875–878.
Yang, J.S., Bai, W.J., Fang, Q.S., Meng, F.C., Chen, S.Y., Zhang, Z.M., Rong, H., 2007b. Discovery of diamond and an unusual mineral group from the podiform chromite, Polar Ural. Chinese Geology 34 (5), 950–952 (in Chinese with English abstract).
Yang, J.S., Bai, W.J., Fang, Q.S., Rong, H., 2008a. Ultrahigh-pressure minerals and new minerals from the Luobusa ophiolitic chromitites in Tibet: a review. Acta Geoscientica Sinica 29 (3), 263–274 (in Chinese with English abstract).
Yang, J.S., Zhang, Z.M., Li, T.F., 2008b. Unusual minerals from harzburgite, the host rock of the Luobusa chromite deposit, Tibet. Acta Petrologica Sinica 24, 1445–1452 (in Chinese with English abstract).
Yang, J.S., Meng, F.C., Xu, X.Z., Robinson, P.T., Dilek, Y., Makeyev, A.B., Wirth, R., Wiedenbeck, M., Griffin, W.L., Cliff, J., 2014. Diamonds, native elements and metal alloys from chromiites of the Ray-Iz ophiolite of the Polar Urals. Gondwana Research 27, 459–485 (in this issue).
Yang, J.S., Xu, X.Z., Li, Y., Li, J.Y., Ba, D.Z., Rong, H., Zhang, Z.M., 2011. Diamond recovered from peridotite of the Purang ophiolite in the Yarlung-Zangbo suture of Tibet: a proposal for a new type of diamond occurrence. Acta Petrologica Sinica 27 (11), 3171–3178 (in Chinese with English abstract).
Yang, J.S., Robinson, P.T., Dilek, Y., 2014. Diamonds in ophiolites. Elements 10, 127–130. http://dx.doi.org/10.2113/gselements.10.2.127.
Zhang, H.Y., Ba, D.Z., Guo, T.Y., Mo, X.X., Xue, J.Z., Ruan, G.P., 1996. Study of Luobusa Typical Chromite Ore Deposit Qusong County, Tibet (Xizang). Xizang People Press, Lhasa, pp. 1–181 (in Chinese).
Zhou, M.F., Robinson, P.T., Bai, W.J., 1994. Formation of podiform chromitites by melt/rock interaction in the upper mantle. Mineralium Deposita 28, 98–101.
Zhou, M.F., Robinson, P.T., Malpas, J., Li, Z., 1996. Podiform chromitites in the Luobusa ophiolite (southern Tibet): implications for melt–rock interaction and chromite segregation in the upper mantle. Journal of Petrology 37, 3–21.
Zhou, M.F., Robinson, P.T., Malpas, J., Edwards, S.J., Qi, L., 2005. REE and PGE geochemical constraints on the formation of dunites in the Luobusa ophiolite, Southern Tibet. Journal of Petrology 46, 615–639.
Zhou, M.F., Robinson, P.T., Su, B.X., Gao, J.F., Li, J.W., Yang, J.S., Malpas, J., 2014. Compositions of chromite, associated minerals, and parental magmas of podiform chromite deposits: the role of slab contamination of contamination of asthenospheric melts in supersubduction zone environments. Gondwana Research 26, 262–283.